Cell

An Immunologic Mode of Multigenerational Transmission Governs a Gut Treg Setpoint

Graphical Abstract

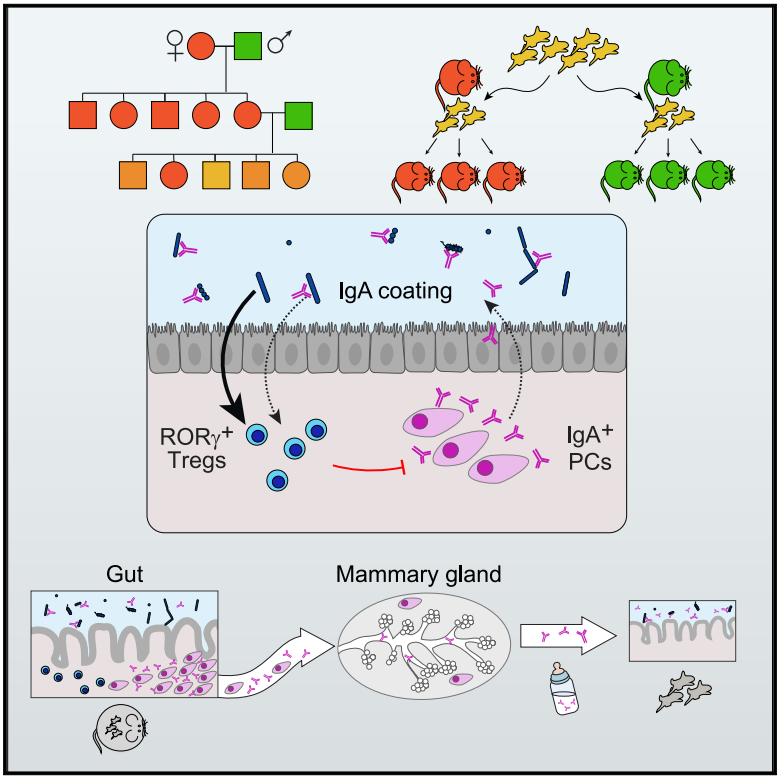

Highlights

- Variations in gut RORγ+ Tregs are maternally transmitted through multiple generations
- RORγ+ Treg setpoint is determined in early life, not driven by genetics or microbiota
- Gut RORγ+ Tregs and IgA form a double-negative regulatory loop
- IgA+ plasma cells expand and migrate in late gestation via the entero-mammary axis

Authors

Deepshika Ramanan, Esen Sefik, Silvia Galván-Peña, ..., Dennis L. Kasper, Diane Mathis, Christophe Benoist

Correspondence

cbdm@hms.harvard.edu (C.B.),
cbdm@hms.harvard.edu (D.M.)

In Brief

The homeostatic level of regulatory T cells in the colon is transmitted across generations and is modulated by maternally transferred IgA.

Ramanan et al., 2020, Cell *181*, 1276–1290
June 11, 2020
https://doi.org/10.1016/j.cell.2020.04.030

CellPress

Cell

Article

An Immunologic Mode of Multigenerational Transmission Governs a Gut Treg Setpoint

Deepshika Ramanan,[1] Esen Sefik,[1] Silvia Galván-Peña,[1] Meng Wu,[1] Liang Yang,[1] Zhen Yang,[2] Aleksandar Kostic,[2] Tatyana V. Golovkina,[3] Dennis L. Kasper,[1] Diane Mathis,[1,*] and Christophe Benoist[1,4,*]

[1]Department of Immunology, Harvard Medical School, Boston, MA 02115, USA

[2]Joslin Diabetes Center and Department of Microbiology, Harvard Medical School, Boston, MA 02115, USA

[3]Department of Microbiology, Committee on Microbiology and Committee on Immunology, University of Chicago, Chicago, IL 60637, USA

[4]Lead Contact

*Correspondence: cbdm@hms.harvard.edu (D.M.), cbdm@hms.harvard.edu (C.B.)

https://doi.org/10.1016/j.cell.2020.04.030

SUMMARY

At the species level, immunity depends on the selection and transmission of protective components of the immune system. A microbe-induced population of RORγ-expressing regulatory T cells (Tregs) is essential in controlling gut inflammation. We uncovered a non-genetic, non-epigenetic, non-microbial mode of transmission of their homeostatic setpoint. RORγ$^+$ Treg proportions varied between inbred mouse strains, a trait transmitted by the mother during a tight age window after birth but stable for life, resistant to many microbial or cellular perturbations, then further transferred by females for multiple generations. RORγ$^+$ Treg proportions negatively correlated with IgA production and coating of gut commensals, traits also subject to maternal transmission, in an immunoglobulin- and RORγ$^+$ Treg-dependent manner. We propose a model based on a double-negative feedback loop, vertically transmitted via the entero-mammary axis. This immunologic mode of multi-generational transmission may provide adaptability and modulate the genetic tuning of gut immune responses and inflammatory disease susceptibility.

INTRODUCTION

The evolution of immunological traits is essential for the fitness of any species. Genome-wide association studies have identified several human genetic variants positively selected for pathogen resistance, but these pathogen-selected genetic variants are a double-edged sword: while buffering populations against widespread epidemics, they increase the risk of autoimmune diseases (Barreiro and Quintana-Murci, 2010). For example, variations in the HLA region that confer protection from or bestow slower progression to tuberculosis and HIV are associated with increased development of rheumatoid arthritis and inflammatory bowel disease (Dendrou et al., 2018). Polymorphisms in genes encoding several cytokines, their receptors, or innate recognition receptors that are crucial for host defense have also been associated with increased autoimmune disease risk (Netea et al., 2012). These polymorphisms are retained in the gene pool, increasing genetic diversity and the overall fitness of a population by balancing selection (Hedrick, 2007). Such variants are widespread in populations, but only a subset of these carriers goes on to develop autoimmune diseases and actually account for only a minor portion of determinism (Ye et al., 2014; Brodin et al., 2015). Hence, identifying the contributions of non-genetic factors is crucial to understand the mechanisms of autoimmune diseases.

While heritability is associated with the genetic make-up of an individual, several phenotypic changes or non-genetic factors are also inherited. These include changes in epigenetic states, where DNA or chromatin modifications acquired in response to environmental cues are passed on from one generation to the other (Allis and Jenuwein, 2016). Parental nutrition states, microbiota composition, metabolites, and behavioral traits are also thought to influence phenotypes and disease susceptibility in offspring (Heard and Martienssen, 2014). But it is unclear to what extent these factors affect the evolution of immunological traits.

Regulatory T cells (Tregs) that express the transcription factor Foxp3 are a unique subset of CD4+ T cells that suppress unwanted innate and adaptive immune responses. Tregs are fundamental in promoting tolerance to harmless antigens, the breakdown of which is considered central to the origin of autoimmune diseases. Tregs are also key players in host-pathogen immunity and tissue healing post infection and inflammation (Schiering et al., 2014). Two distinct subpopulations of intestinal Foxp3$^+$ Tregs are distinguished by their expression of the transcription factors Helios or RORγ. RORγ+ Tregs constitute the major subset of colonic Tregs and differentiate locally in response to bacterial antigens from 15–20 days of age onward (Sefik et al., 2015; Ohnmacht et al., 2015). Individual microbes, even members of the same bacterial genus, vary widely in the

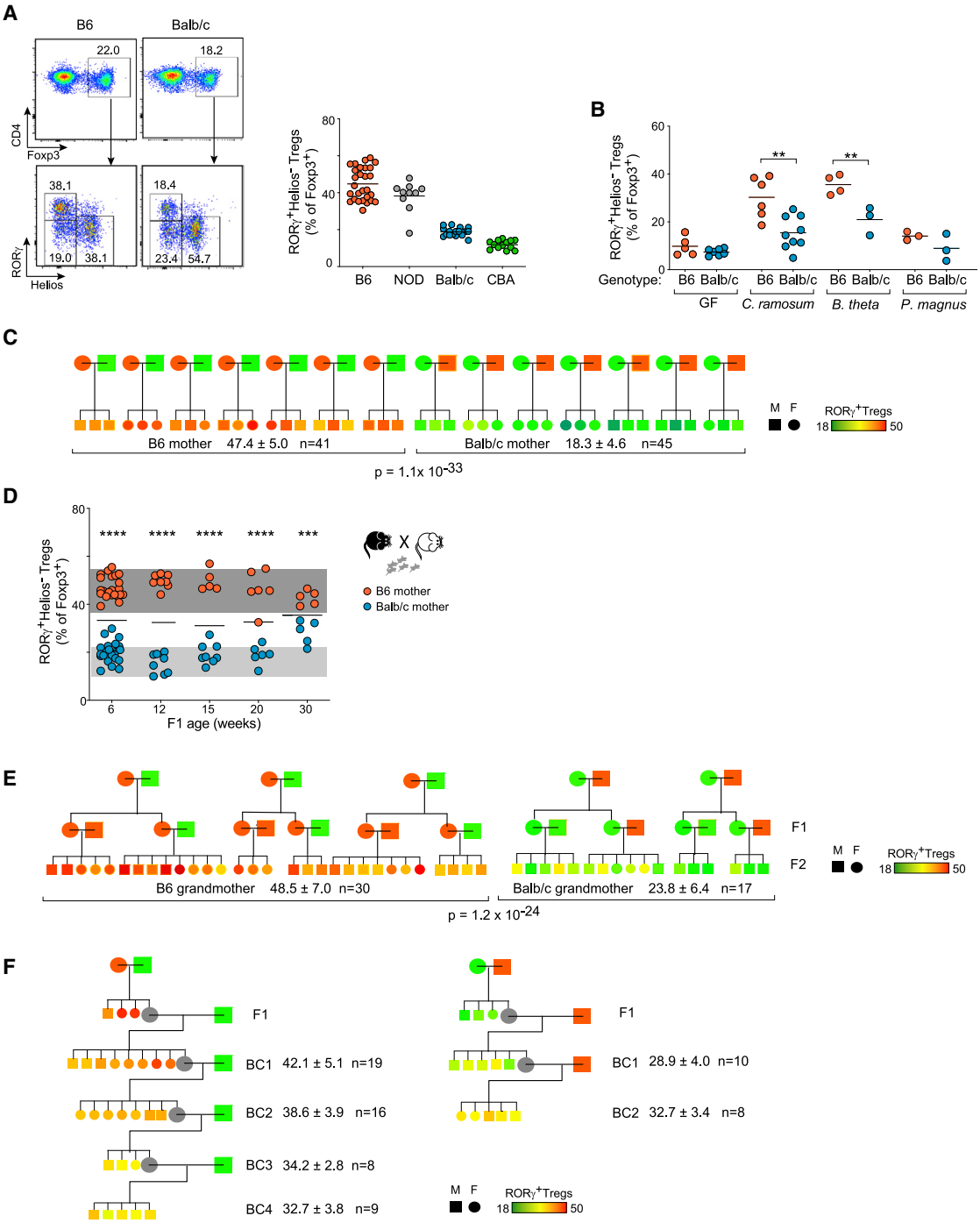

Figure 1. Proportions of Colonic RORγ+ Tregs Are Different in Inbred Mouse Strains and These Proportions Are Determined Maternally

(A) Proportions of colon RORγ+ Tregs in different inbred mice, gated as shown in left.

(B) Proportions of colon RORγ+ Tregs in GF B6 or BALB/c mice monocolonized with indicated microbes. (throughout t test p value, **p < 0.01; ***p < 0.001; ****p < 10^{-4}).

(C) Representative pedigree chart showing colon RORγ+ Treg proportions (color-coded as indicated; sex denoted by shape) in F1 offspring of B6 and BALB/c mothers (for space, only 3 representative F1s are shown for each of 14 breeding pairs, all values summarized).

(D) Proportions of RORγ+ Tregs in (B6 × BALB/c) F1 offspring at different ages. Shading indicates the usual range of RORγ+ Tregs in B6 and BALB/c mice.

(legend continued on next page)

proportions of RORγ+ Tregs they induce (Sefik et al., 2015), through several potential mechanisms (Verma et al., 2018; Yissachar et al., 2017; Hang et al., 2019; Song et al., 2020). Mice deficient in RORγ+ Tregs display microbial dysbiosis and increased inflammatory Th17 cells and are more susceptible to colitis in different models (Sefik et al., 2015; Ohnmacht et al., 2015; Xu et al., 2018; Al Nabhani et al., 2019; Neumann et al., 2019; Ye et al., 2017). Microbe-specific development of RORγ+ Tregs around weaning is critical to dampen susceptibility to colitis and colorectal cancer (Al Nabhani et al., 2019). Patients with food allergies have fewer RORγ+ Tregs, and commensal-bacteria-mediated protection from food allergies is dependent on RORγ+ Tregs (Abdel-Gadir et al., 2019). Increasing proportions of RORγ+ Tregs could be beneficial in preventing inflammation, but there seems to be a homeostatic control of the levels of RORγ+ Tregs in mice, where manipulating germ-free (GF) or specific-pathogen-free mice (SPF) with high inducers of RORγ+ Tregs does not push its levels beyond a pre-established ceiling (Geva-Zatorsky et al., 2017). Hence, the mechanisms that regulate the homeostatic balance between Helios+ and RORγ+ Tregs are largely unknown.

Here, in exploring the homeostatic control of RORγ+ Treg levels in inbred mouse strains, we uncovered a mammalian example of non-genetic inheritance of an immunological trait through multiple generations. We report a novel mode of transmission of maternal factors via the entero-mammary axis that influences colonic Treg differentiation and function and sets the immunoregulatory tone in the intestine through generations.

RESULTS

Strain-Specific and Unusual Transmission of RORγ+ Treg Frequencies

Variation between inbred strains has been a useful handle to approach cell function. To better understand RORγ+ Treg differentiation and function, we analyzed colonic Tregs in several inbred strains of mice. On the B6 background, RORγ+ Tregs constituted a substantial proportion (40%–60%) of colonic Tregs, per Sefik et al. (2015) and Ohnmacht et al. (2015), but lower frequencies were observed in BALB/c and CBA/J mice with a compensatory increase in Helios+ Tregs (Figure 1A). RORγ+ Tregs express high levels of c-Maf, which is important for their differentiation and stability (Xu et al., 2018; Neumann et al., 2019). The genetic difference also applied to c-Maf+ colonic Treg cells (Figure S1A). The difference between B6 and BALB/c was reproducible with mice from different vendors (Figure S1B), suggesting a stable genetic trait rather than environmental variables. To verify this point, we monocolonized GF B6 and BALB/c mice with *Clostridium ramosum* or *Bacteroides thetaiotamicron*, microbes that induce high RORγ+ Treg frequencies (Sefik et al., 2015). While RORγ+ Tregs were induced by these microbes (but not by *Peptostreptococcus magnus*, a control) in both GF strains, the inter-strain differences remained strong (Figure 1B), confirming that a non-microbial element controlled inter-strain variance in RORγ+ Tregs.

To map the transmission of this trait, we intercrossed RORγ+ Treg-high and RORγ+ Treg-low strains, yielding B6 × BALB/c F1 mice. Oddly, colonic RORγ+ Tregs in adult F1s followed a bimodal distribution, which we realized tracked with the mother's genotype: high RORγ+ Treg frequencies in F1 mice born to a B6 dam, low if to a BALB/c dam (Figure 1C; Table S1). This partition was found in 86 offspring of either sex from 14 independent breeding pairs ($p < 1.11 \times 10^{-33}$), establishing that the RORγ+ Treg trait was maternally transmitted. The proportions of Helios+ Treg changed in balance (Figure S1C), but the overall proportions of FoxP3+ Tregs were unaffected by maternal type (Figure S1D). This maternal dominance was visible even though fathers were routinely left in the breeding cages. Maternal transmission was also observed in high × low intercrosses between three other strain combinations (Figures S1E–S1G), showing that the phenomenon was not a peculiarity of the B6 or BALB/c strains, but a general one. When both B6 and BALB/c mothers were co-housed in a cage with all of their progeny, the pups acquired high RORγ+ Treg frequencies, indicating that the high RORγ+ Treg phenotype prevailed, although BALB/c offspring never quite reached the levels seen in co-fed B6 offspring (Figure S1H). Once established, the maternally transmitted difference remained long-term in F1 mice (Figures 1D and S1E–S1G).

To determine whether the maternally derived trait could be further transmitted, we bred and analyzed F2 mice by intercrossing F1 females and males. Remarkably, the progeny of the F1 crosses again mirrored the RORγ+ Treg phenotype of their mothers—and thus grandmothers, irrespective of their father's origin (Figure 1E). Furthermore, the maternally transmitted trait was carried through several generations of backcross against males of the opposite parental genotype (Figure 1F). There was a trend toward reversion to the genetic type after a few generations ($p < 10^{-7}$), likely reflecting a gradual transition of the non-genetic maternal influence combined with a genetic shift. Thus, inter-strain variance in colonic RORγ+ Treg frequency was determined via matrilineal transmission, in an unusual gene × environment interaction where mothers provided both the genes and the environment.

RORγ+ Treg Proportions Were Determined during an Early Postnatal Window

These results raised the question of the identity of the maternal factor, epigenetic or other, responsible for the transmission. Colonic RORγ+ Tregs are absent during the first two weeks after birth and appear only between 15 and 20 days of age. Their appearance coincides with profound changes in the microbiota associated with weaning and the transition to solid food (Al Nabhani et al., 2019), but also results from an intrinsic change in the

(E) Pedigree chart of colon RORγ+ Tregs (color code and sex as in C) in F2 mice resulting from crossing (B6 × Balb/c) F1 females to (B6 × Balb/c) F1 males as shown.

(F) Representative pedigree chart of multiple generation backcross of (B6 × Balb/c) F1 females against BALB/c (left) or B6 (right) males, females for breeding picked randomly. Representative colonic RORγ+ Tregs at 6 weeks of age in non-bred littermates are shown (unknown in breeder females).

Data representative of >3 independent experiments, bars in plots indicate mean.

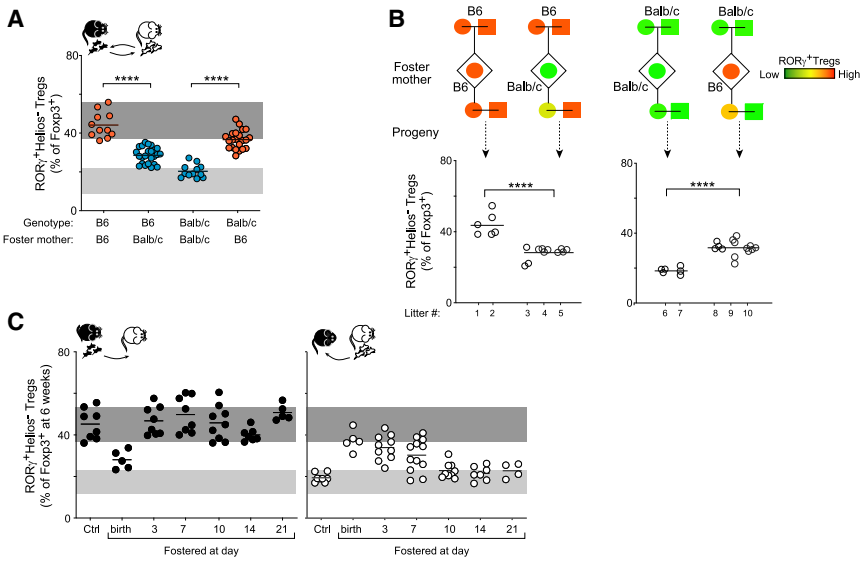

Figure 2. RORγ+ Treg Proportions Are Maternally Imparted during an Early Neonatal Window, and the Learned Phenotype Is Transferable

(A) Proportions of RORγ+ Tregs at 6 weeks of age in B6 or BALB/c mice fostered at birth by BALB/c or B6 mothers, compiled from 6 different litters (*t test ****$p < 10^{-4}$). Shading indicates the usual range of RORγ+ Tregs in B6 and BALB/c mice.

(B) Top: experimental schematic. B6 or BALB/c females were fostered at birth by a B6 or BALB/c mother, and later crossed to a syngeneic male. Bottom: colon RORγ+ Tregs were quantitated in their offspring at 6 weeks of age (t test ****$p < 10^{-4}$). Data compiled from 3 litters, as indicated.

(C) B6 mice were fostered by BALB/c mothers (left) or the reverse (right) starting at birth or at indicated ages, and their RORγ+ Tregs quantitated at 6 weeks of age. Shading as above.

Data representative of >3 independent experiments, bars in plots indicate mean

T cell pool from which colonic Tregs derive (Pratama et al., 2020). To define the developmental stage at which RORγ+ Treg proportions were maternally transmitted, we cross-fostered B6 and BALB/c pups at birth (here, and in all other experiments in this paper, colonic Tregs were profiled at 6 weeks of age, unless stated otherwise). The mice showed RORγ+ Treg proportions similar to that of their foster mothers than to their birth mothers (Figure 2A). This observation excluded the possibility that matrilineal transmission resulted from epigenomic imprinting, mitochondrial DNA, or immunological modifications imparted during gestation (Gomez de Agüero et al., 2016; Kim et al., 2017; Sharon et al., 2019). However, mice cross-fostered onto the opposite genotype did not quite reach the setpoints of purebred mice, indicating a complex gene × environment effect. We quantitated the relative contributions of components transmitted by the foster mother versus the genetic component by fitting a linear model to these data. The foster mother's genotype contributed 60.7% of the variance ($p < 10^{-7}$) versus 27.3% of variance for the pup's genetic component ($p < 10^{-6}$). As for maternal transmission in the F1 context, the transmitted trait was stable and could be further transmitted by females to their own progeny, even when crossed with males of their own genotype (Figures 2B and S2A), producing offspring with pure B6 genomes but with low colonic RORγ+ Treg proportions similar to those of a BALB/c mouse (and vice versa), although not quite reaching the parental level, again indicating a compound maternal plus genetic determinism.

Experiments in which we delayed the age of cross-fostering showed that the time window for maternal transmission of the RORγ+ Treg trait was very narrow. If fostered by BALB/c mothers, B6 pups could no longer acquire the low phenotype after 3 days of age, implying that their birth mother had marked them during those first 3 days. For BALB/c pups, the high phenotype could be acquired from B6 foster mothers up to days 3–7, but not later (Figure 2C). Thus, maternal exposure and feeding during the first few days of life set the tone for RORγ+ Treg frequencies in adults. This time window is distinctly earlier than the appearance of RORγ+ Tregs, microbiota changes at weaning, and accompanying perturbations (Al Nabhani et al., 2019).

Maternal Transmission Affects the Response to Infection

Several lines of evidence demonstrate that RORγ+ Tregs have non-redundant roles in controlling various facets of immunologic activity in the gut, but it was important to establish the functional relevance of their maternally controlled variance. We thus studied a model of intestinal infection involving the mouse pathogen *Citrobacter rodentium*, infecting adult B6 mice that had been cross-fostered by either B6 or BALB/c mothers. Compared with mice fostered by B6 mothers, those fostered by BALB/c mothers had less severe colitis (Figure 3A), with lower bacterial burdens in the gut (Figure 3B) and decreased bacterial translocation to extra-intestinal sites (Figure 3C). Conversely, they showed an increase in interleukin-17 (IL-17)-producing and interferon-γ (IFN-γ)-producing colonic T cells (Figure 3D), known to be protective against *C. rodentium* infection (Collins et al., 2014). Thus, in these genetically identical mice, maternally determined high levels of RORγ+ Tregs correlated with dampened anti-bacterial inflammatory responses. Although parallel causality cannot be ruled out, the data are compatible with the notion that maternally determined variations in RORγ+ Tregs frequencies can directly impact infection outcome.

Resistance to Perturbation of the Maternally Transmitted Phenotype

Because RORγ+ Tregs appear 2 weeks after the narrow postnatal window of maternal transmission, the maternal effect thus determined the homeostatic setpoint of colonic RORγ+ Tregs for the mouse's future rather than immediately inducing the cells. Plausible hypotheses for how the setpoint was imprinted by the mothers are that it could be controlled by the Treg pool, by the microbiota, or by adaptations in the local microenvironment (stroma, immune cells). We tested these hypotheses by perturbing each element. First, we cross-fostered

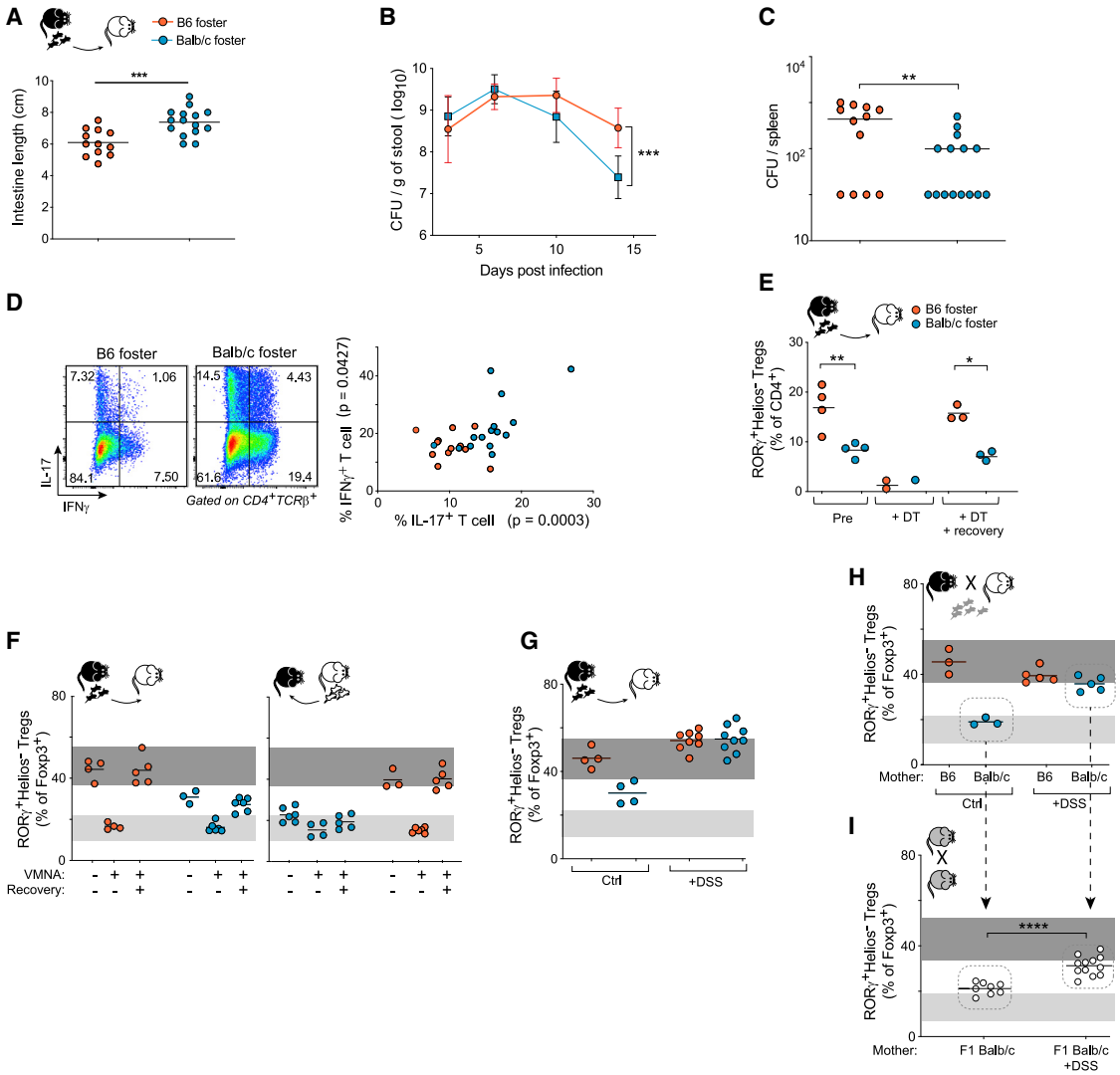

Figure 3. Impact and Stability of the Maternally Transmitted RORγ+ Treg Setpoint

(A–D) B6 mice fostered at birth by B6 or BALB/c mothers were infected with 10^9 cfu of *C. rodentium* at 6 weeks of age. (A) Intestine length after 2 weeks (t test ***p < 0.001); (B) *C. rodentium* counts in stool over the course of infection (t test ***p < 0.001, mean ± SD) and (C) in spleen on day 15 (Mann-Whitney **p < 0.01); (D) flow cytometry plots of IFN-γ− and IL-17-producing colonic CD4+ T cells, quantitated at right (t test p values).

(E) B6 *Foxp3*^{DTR} mice were fostered by B6 or BALB/c mothers at birth; colon RORγ+ Tregs were quantitated at 6 weeks of age (Pre), after two doses of DT, or after 4 weeks recovery (t test *p < 0.05, **p < 0.01).

(F) B6 and BALB/c mice were fostered by B6 or BALB/c mothers at birth; colon RORγ+ Tregs were quantitated at 6 weeks of age, after antibiotic treatment (VMNA) for 3 weeks, or after 4 weeks recovery.

(G) B6 mice fostered by B6 or BALB/c mothers at birth were treated with 2.5% DSS in drinking water for 6 days at 7 weeks, and colon RORγ+ Tregs analyzed 10 days post treatment.

(H) F1 females born to B6 or BALB/c mothers were treated with 4% DSS in drinking water for 6 days at 7 weeks and RORγ+ Tregs analyzed 10 days post treatment.

(I) Some of their similarly treated littermates were then bred to naive F1 males, and RORγ+ Tregs analyzed in their 6-week-old progeny (t test ****p < 10^{-4}). Data representative of >3 independent experiments, bars in plots indicate mean.

neonates from the *Foxp3*^{DTR} lineage ablation line (B6 background) by either B6 or BALB/c females. Fostering on lactating B6 and BALB/c females led to high and low RORγ+ Tregs as expected (Figure 3E). Most Tregs disappeared from the colon after transient diphtheria toxin (DT) treatment (<3% remaining). When Tregs recovered after 4 weeks, RORγ+ Tregs also returned to their preset proportions (Figures 3E and S2B). Thus, the maternally inherited Treg trait survived transient Treg ablation, suggesting that it was not autonomous to the mature Treg pool itself, but present in their precursors or colonic environment.

Second, to test whether changing the microbial niche could alter the RORγ+ Treg phenotype, we treated adult mice, which

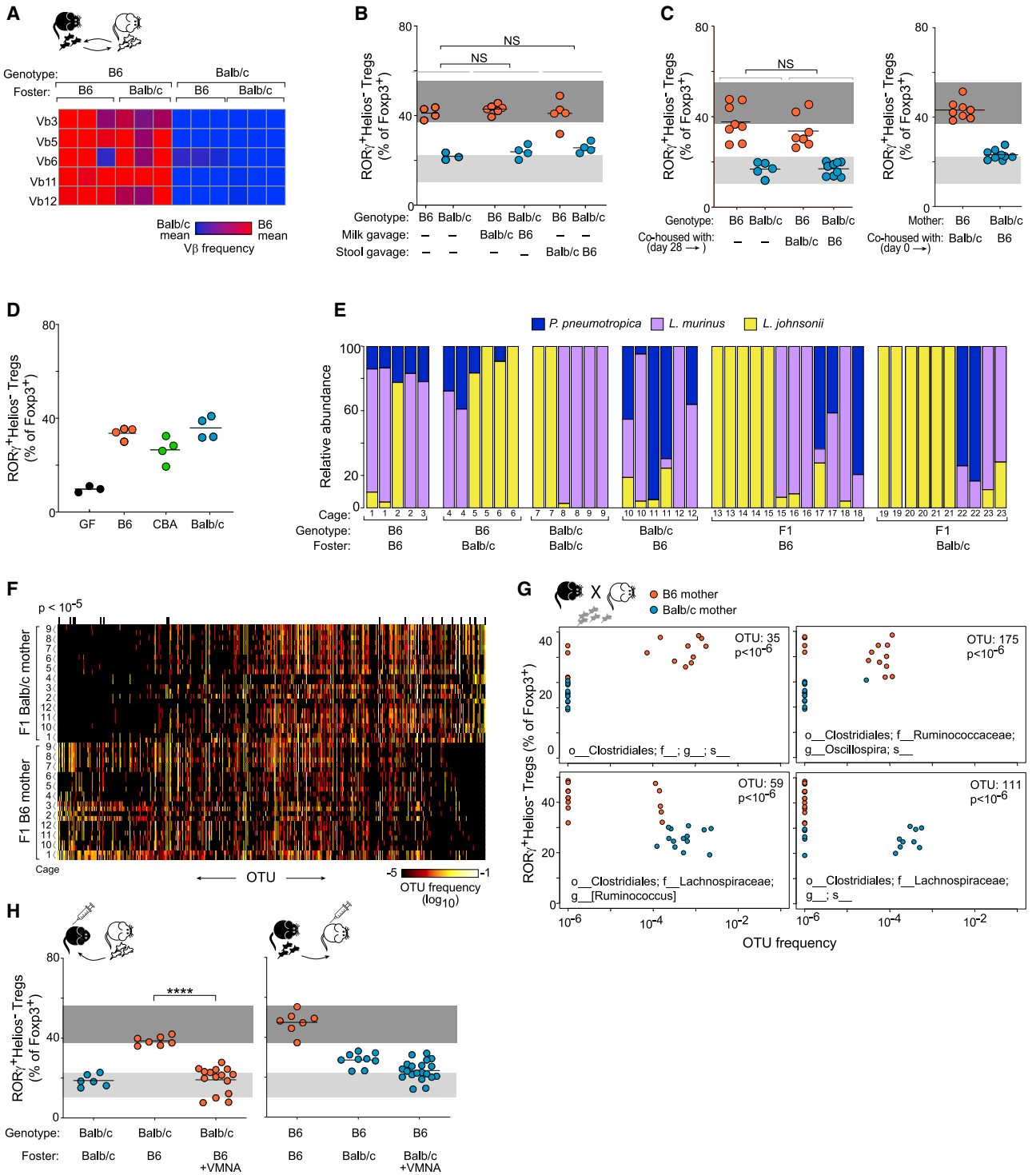

Figure 4. Maternal Transfer of RORγ+ Treg Proportions Is Not Dependent on Transmission of Specific Microbial Taxa

(A) Relative frequencies of TCR Vβ usage in splenic CD4+ T cells from B6 or BALB/c mice fostered by BALB/c or B6 mothers at birth.

(B) Proportions of RORγ+ Tregs in 6-week-old B6 and BALB/c mice that received, as neonates (housed with birth mother), milk or stool from BALB/c and B6 females in the first 3 days of life.

(C) RORγ+ Tregs in 6-week-old B6 and BALB/c mice co-housed at 28 days of age for 2 weeks (left) or on the day of birth with adult virgin B6 or BALB/c females (right).

(D) RORγ+ Tregs in GF mice colonized with stool from adult B6, CBA/J, or BALB/c SPF mice for 2 weeks.

(legend continued on next page)

had been cross-fostered at birth, with a cocktail of broad-spectrum antibiotics (VMNA) to clear intestinal microbes and reduce RORγ+ Tregs (Sefik et al., 2015; Ohnmacht et al., 2015) (Figure 3F). Again, after 4 weeks of recovery, RORγ+ Tregs returned to their original setpoint. Thus, the maternally transmitted trait seemed to resist a profound shuffling of the microbiota.

Third, we asked whether perturbations of the intestinal environment could affect the phenotype, using dextran sodium sulfate (DSS), which induces epithelial damage and strong colonic inflammation. Here, treatment did affect RORγ+ Treg proportions, which became high regardless of the mother, in both cross-fostered (Figures 3G and S2C) and F1 mice (Figure 3H). Importantly, this newly acquired Treg setpoint was stable and transmissible: offspring of DSS-treated F1 mice had significantly higher proportions of RORγ+ Tregs than offspring of untreated mice (Figure 3I). These results suggest that the RORγ+ Treg phenotype could be imprinted in neonates and maintained thereafter, in spite of complete Treg or microbiota resetting, but that major damage to the intestinal wall and resulting inflammation can reset the setpoint, for the animal and its descendants.

Mediators of the Maternal Transmission of RORγ+ Treg Phenotype?

The central issue to address was what the mothers were actually transmitting during this narrow postnatal window that set the tone for colonic Tregs. B6 and BALB/c strains have different metabolic parameters, most markedly evidenced by body weights that were influenced by the mothers of F1 mice. However, body weights were clearly unrelated to the difference in RORγ+ Treg proportions (Figure S3A; 0.9% of variance and $p = 0.18$, versus 95.9% of variance and $p < 10^{-7}$ for maternal genotype in a linear model), nor were litter size–which affect how much nutrition each pup receives (Figure S3B).

Vertical transmission of microbes from mothers to offspring has been well documented (Moon et al., 2015; Ferretti et al., 2018; Yassour et al., 2018; McDonald and McCoy, 2019), and, although the points mentioned above argued against a mere transmission of microbiota, we revisited this possibility. One plausible scenario was the milk-borne transmission of endogenous retroviruses, in particular of the MMTV family, whose superantigens induce clonal deletion of T cells and affect their responsiveness (Marrack et al., 1991; Acha-Orbea and MacDonald, 1995). T cell receptor (TCR) Vβ profiling of spleen and colon T cells showed the expected differences between B6 and BALB/c mice (e.g., reduction of the Mtv-sensitive Vβ3, 5, 6, 11, and 12), but cross-fostering at birth had no effect, as the mice kept their genetically determined Vβ patterns (Figure 4A). We also detected no infectious ecotropic, polytropic, or xenotropic murine leukemia viruses by plaque assay, ruling out the role of dominant milk-borne viruses in the maternal transmission of colonic Treg phenotypes.

We then tested whether the mothers were transferring, via stool or milk, a microbial agent that would colonize the neonates. We gavaged B6 and BALB/c pups for 3 days after birth with feces or milk from BALB/c or B6 postpartum females. This treatment did not change their later RORγ+ Treg phenotype (Figure 4B). These data suggest that the transmission of a dominant microbe does not overcome the effect of the birth mother still in the cage.

Several other lines of evidence argued against the hypothesis that variations in microbes transmitted from the mother might lead to differential establishment of colonic Treg pools. First, classic co-housing of adult B6 and BALB/c mice never resulted in any change in RORγ+ Treg frequencies (Figure 4C, left), nor did adding a virgin female of the opposite genotype together with lactating females (Figure 4C, right) (fathers were also routinely left in the F1 breeding cages, to no effect). Second, colonization of GF mice with stool from adult inbred mice of high or low RORγ+ Treg phenotype resulted in similarly high RORγ+ Treg levels (Figure 4D), indicating that microbes from low strains like CBA and BALB/c were quite capable inducers (as expected from the large proportion of bacterial strains that can elicit such responses; Sefik et al., 2015). Finally, we used 16S and metagenomic profiling to test directly whether the genotype of the mother modified the gut microbiomes of their offspring in F1 intercrosses or during cross-fostering. In 3-day-old neonates, the gut microbiota was extremely simple as expected (Yatsunenko et al., 2012; Knoop et al., 2015), dominated by *Lactobacilli* (*murinis* or *johnsonii*) and *Prevotella pneumotropica* (Figure 4E). Although these species varied widely, their distribution reflected cage-of-origin effects but neither the pups' nor the foster mothers' genotypes, thus unrelated to the transmitted Treg trait. In adults, a first metagenomic analysis of fecal bacterial populations in F1 or cross-fostered mice revealed no species or pathway significantly associated with maternally determined bias (Figures S3C and S3D). For increased power, we performed 16S fecal rDNA profiling on another 48 F1 mice from either B6 or BALB/c mothers (24 independent breeding cages, Table S2). Differential representation analysis, or a random forest classification procedure, did identify a few taxons (all *Clostridiales*) with differential representation in F1 mice from B6 or BALB/c mothers, which permutation testing showed to be significant, beyond strong cage-of-origin effects (Figures 4F and S3E; Table S2). However, their relative frequencies in individual mice was unrelated to Treg proportions (Figure 4G). In addition, pairwise UniFrac distances are much closer between mice that share a

(E) Neonate microbiota: relative abundance of bacterial species in stool from 3-day-old mice (metagenomic analysis). Mice were B6 or BALB/c pups cross-fostered onto B6 or BALB/c mothers or F1s from B6 or BALB/c mothers.

(F) Adult microbiota: bacterial population analysis (16S rDNA) on 24 + 24 6-week-old F1 mice from B6 or BALB/c mothers (each from 12 breeding cages). Frequencies for the 545 OTUs with frequencies $>10^{-5}$ in at least 5 samples are shown, ordered by the mean differential representation in offspring of B6 or BALB/c mothers. OTUs with KS test for B6 versus BALB/c origin $p < 10^{-5}$ marked at top).

(G) 4 representative OTUs from (F). Frequency in stool of F1 mice from B6 or BALB/c mothers plotted against RORγ+ Treg proportions, each dot an individual mouse. KS test for B6 versus BALB/c origin is shown.

(H) RORγ+ Treg proportions after reciprocal fostering at birth, where pregnant foster mothers were treated with broad-spectrum antibiotics (VMNA, 2–5 days before delivery) ****t test $p < 10^{-4}$.

Data representative of >3 independent experiments, bars in plots indicate mean

cage than those that merely share a maternal genotype (Figure S3E), which contrasts with the segregation of the Treg phenotype (no cage-of-origin effect). Thus, while B6 or BALB/c mothers do preferentially pass on different microbiota (particularly *Clostridiales*) to their offspring, this appears unrelated to the Treg phenotype.

While microbes are required to induce RORγ+ Tregs (Sefik et al., 2015; Ohnmacht et al., 2015), the maternally transmitted phenotype was not manifestly dependent on a single microbe or a defined group of microbes. To resolve this apparent contradiction, we treated pregnant B6 and BALB/c females with VMNA for the last 5 or 2 days of gestation, and asked whether they could still transmit their phenotype to fostered newborns. Antibiotic-treated B6 mothers were no longer able to transfer their high phenotype to their foster BALB/c pups but treated BALB/c mothers could still reduce levels in their B6 fosters (Figure 4H). This split suggests that the presence of microbes was important in determining the high RORγ+ Treg phenotype in the first days of life, even if the microbiota itself was not the differentially transmitted trait (Figure 4H).

Maternally Controlled Immunologic Correlates of RORγ+ Tregs

As an alternative approach to identify the mechanism of maternal transmission, we immuno-profiled colon lamina propria (LP) cells in B6xBalb/c F1 progeny and cross-fostered mice. In both 3-day-old neonates and 6-week-old adults, the majority of lymphoid or myeloid populations proved to be unaffected by maternal transmission (Figure S4; Table S3), including CX3CR1+ DCs, which have been associated with RORγ+ Treg differentiation (Solomon and Hsieh, 2016). There were maternally influenced differences in type 2 and type 3 innate lymphoid cells (ILCs) in 3-day-old pups, but these differences did not persist in adults (Figure S5A; Table S3). On the other hand, we detected two traits with clear evidence of maternal transmission and prolonged stability. First, judging from a panel of activation markers, the activation status in LP CD4+ T cells was higher in adult F1 mice born to B6 than to BALB/c mothers, most clearly in conventional T cells but also in RORγ+ Tregs (Figure 5A; Table S3). Second, adult F1 mice born to BALB/c mothers had significantly higher frequencies of immunoglobulin A (IgA)+ B220− plasma cells in the colon and small intestine (but not Peyer's patches or bone marrow) than did those from B6 mothers (Figures 5B and S5B), which was associated with high IgA in stool and serum (Figure 5C). Correspondingly, the coating of stool bacteria by IgA, but not IgG, was also different in F1 mice of both origins (Figures 5D and S5C), with an inverse correlation with RORγ+ Treg frequencies. This difference in IgA did not entail differences in T follicular helpers in the Peyer's patches (Figure S5D) as reported in other contexts (Koch et al., 2016; Hirota et al., 2013). The negative correlation between RORγ+ Treg and IgA production extended to other inbred strains (Figure 5E). Bacterial coating by IgA in adult mice reflects their own ability to produce IgA. Interestingly, similar differences were detected in 3-day-old neonates, at a time when all gut IgA is of maternal origin (Figure 5F, left), whether in F1 or in cross-fostered pups (Figure 5, right), and in keeping with the different IgA content of B6 and BALB/c milk (Figure 5G). Thus, the IgA received from its mother seems to be a harbinger of a mouse's IgA production and coating of bacteria as an adult. We have not formally shown that milk transfer alone can result in IgA differences, which would be technically daunting (neonates must be fed every 2 h), but we infer that milk must be the vector of maternal transmission by elimination of other options (Figure 5).

Importantly, the IgA coating phenotype set by the mother was then transmissible by females to their own offspring, with a multigenerational pattern of maternal transmission strikingly similar to that of RORγ+ Treg levels (Figure 5H), including the same trend of reversion to the genetic type after several generations. Thus, the proportions of colonic RORγ+ Tregs and IgA+ plasma cells (and the degree of IgA coating of gut microbes) were inversely correlated, both learned during the postnatal period, and maternally transmitted through multiple generations.

Amplification and Migration of IgA+ Plasma Cells in Late Pregnancy

Next, we explored the entero-mammary axis, or how variations in gut IgA might be reflected in the milk and result in multi-generational transfer of the IgA setpoint. First, we measured IgA+ plasma cells in the intestine and mammary gland of B6 mice during pregnancy and at different stages of lactation. There was a strong expansion (6-fold on average) of intestinal IgA+ plasma cells in pregnant females (E18.5) compared with virgins (V), which continued during the first few days of lactation (Figure 6A). This expansion was also reflected in the mammary gland (Figure 6A). During pregnancy and lactation, intestinal plasma cells are thought to migrate to the mammary gland, and then contribute to milk Ig (Roux et al., 1977; Wilson and Butcher, 2004). We tested the migration of plasma cells from the gut to the mammary gland using Kaede photoconvertible reporter mice, which we used previously to assess migration from the gut to other tissues by photoconverting intestinal tissues and searching for migrated lymphocytes at later time-points (Tomura et al., 2008; Morton et al., 2014). We generated Kaede+ (B6xBalb F1) females, who were impregnated. Sections of their intestines were photoconverted on the day of birth, and mammary glands analyzed 48 h later for photoconverted red cells of gut origin (Figure 6B). Cells that had migrated from the gut were indeed detected in the mammary glands at L3 (Figure 6C), and in numbers equal or greater to those homing to the spleen or the bone marrow (Figure 6D). Thus, late pregnancy is accompanied by an upsurge in the number of intestinal plasma cells, which traffic actively to the mammary gland.

We then compared the migration of IgA+ plasma cells with the mammary glands of F1 mothers who themselves had B6 or BALB/c mothers. No significant difference was seen (Figure 6E), which was consistent with the comparable numbers of IgA+ plasma cells present in mammary glands of these F1 mice (Figure 6F). On the other hand, despite these similar rates of entero-mammary migration, milk IgA was significantly higher in F1 mice originating from BALB/c versus B6 mothers (Figure 6G), which we conclude must arise from differences in circulating IgA protein rather than migrating cells.

RORγ+ Tregs and Secretory IgA Form a Double-Negative Feedback Loop, which Is Transferred Maternally through the Entero-Mammary Axis

These observations led us to consider the model illustrated in Figure 7A, which incorporates our results with findings from prior

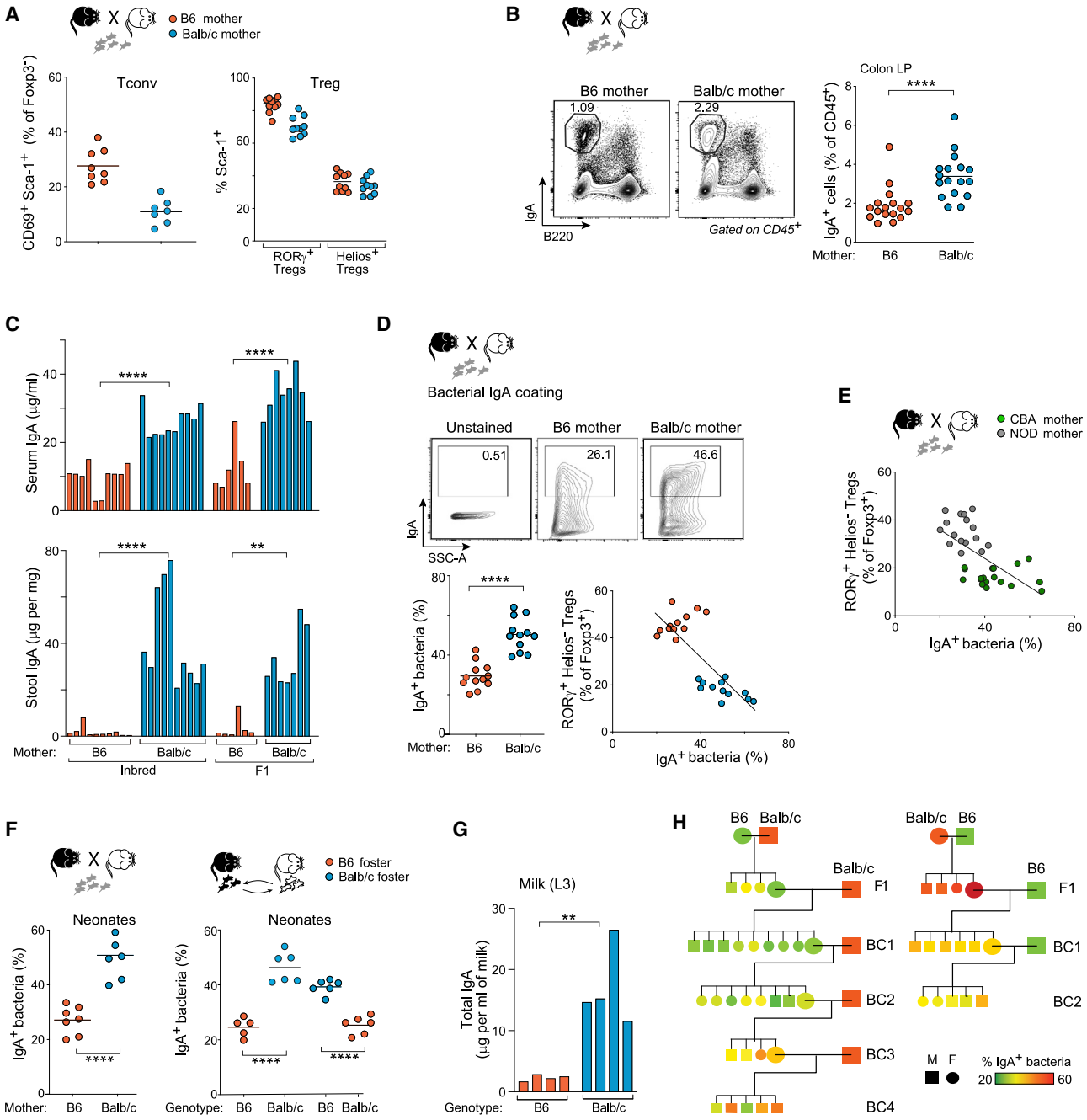

Figure 5. Immuno-Profiling Reveals that F1 Mice Born to B6 and BALB/c Mothers Display Differences in Their T Cell Activation States and IgA Levels

(A) Frequency of conventional T cells expressing the activation markers CD69 and Sca-1 (left), and of RORγ+ or Helios+ Treg cells expressing Sca-1 (right) in adult F1 mice born to B6 or BALB/c mothers.

(B) Representative flow cytometry plots and quantification of colonic IgA+ B220– plasma cells in adult F1 mice (throughout t test, $^{**}p < 0.01$, $^{****}p < 10^{-4}$).

(C) Total IgA (ELISA) in serum (top) and stool (bottom) of 6-week-old B6 mice, BALB/c mice, and F1 mice born to B6 or BALB/c mothers.

(D) Representative flow cytometry plots (top) and quantification (bottom left) of IgA-coated bacteria in stool of adult F1 mice born to B6 or BALB/c mothers, and correlation with colonic RORγ+ Tregs (bottom right).

(E) Correlation plot between colonic RORγ+ Tregs and IgA-coated bacteria in stool of adult F1 mice born to CBA or NOD mothers.

(F) Proportions of IgA coated bacteria in 3-day-old F1 mice born to B6 or BALB/c mothers (left) and in 3-day-old B6 or BALB/c pups fostered by BALB/c or B6 mothers at birth (right).

(G) Total IgA (ELISA) in milk from B6 or BALB/c mothers at day 3 of lactation.

(H) Proportion of IgA-coated bacteria in representative mice from the backcross pedigrees of Figure 1F (color-coded as indicated; sex denoted by shape).

Data representative of >3 independent experiments, bars in plots indicate mean

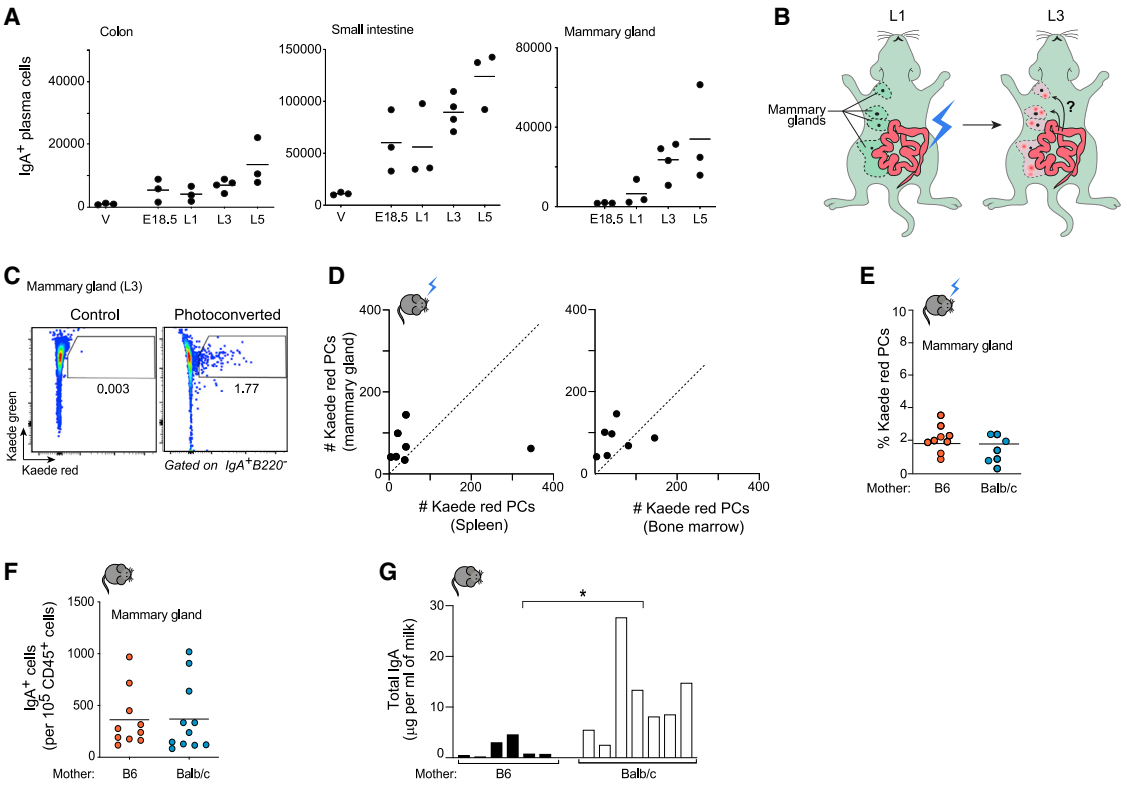

Figure 6. Expansion and Migration of IgA+ Plasma Cells

(A) Number of IgA+ plasma cells in the colon, small intestine, and mammary gland of B6 mothers during late gestation (E18.5) or early days of lactation (L1–L5) versus virgin controls (V).

(B) Experimental design: intestines of Kaede+ mice were photoconverted (green to red) by illumination after laparotomy on day L1, and migration of cells to the mammary gland examined 48 h later (L3).

(C) Representative plots of mammary gland plasma cells at L3 for Kaede green (baseline) versus red (result of illumination of the intestine at L1) in a non-photoconverted versus photoconverted mouse.

(D) Numbers of migrated Kaede red plasma cells of gut origin, 48 h after intestinal illumination, in the mammary gland, spleen, or bone marrow of L3 females.

(E) Proportion of Kaede red plasma cells of gut origin in the mammary gland of L3 F1 females from B6 or BALB/c mothers.

(F) Total number of IgA+ plasma cells in the mammary glands at L3 of F1 females from B6 or BALB/c mothers.

(G) Total IgA (ELISA) in milk at L3 of F1 females from B6 or BALB/c mothers (t test, *$p < 0.05$).

Data representative of >3 independent experiments, bars in plots indicate mean

reports (Neumann et al., 2019; Wilson and Butcher, 2004; Roux et al., 1977): RORγ+ Tregs and IgA reciprocally inhibit each other in adult mice. High levels of IgA and bacterial IgA coating established after birth set the balance that will be maintained during the life of the animal. This balance in the gut then determines the level of IgA that the female will pass on to her own progeny, thus creating a multi-generational transmission loop. We attempted to test the key tenets of this model.

Do RORγ+ Tregs inhibit IgA+ plasma cells, or the reverse, or both? First, we bred paired Ig-deficient BALB/c.*Jh*−/− and wild-type BALB/c.*Jh*+/+ female littermates, impregnated them, and used them to foster splits of B6 litters. Remarkably, adult B6 mice that had been fostered by a BALB/c.*Jh*−/− mother had high proportions of RORγ+ Tregs and low IgA coating of their intestinal microbes, unlike those fostered by a wild-type BALB/c female (Figure 7B). The same relationship was observed in F1 mice derived from BALB/c.*Jh*−/− mothers, who acquired RORγ+ Treg and IgA proportions similar to those of F1 mice derived from B6 mothers (Figures 7C and S5E). The Ig status of the mothers also influenced the activation states of colonic Tregs in F1 offspring (Figure S5F). Finally, to ensure that these effects were indeed linked to IgA, we compared F1 mice born from BALB/c.*Iga*−/− or WT BALB/c mothers. Here again, RORγ+ Tregs in the F1 offspring of IgA-deficient mothers were comparable with those of mice born of B6 mothers (Figure 7D). Thus, IgA received at birth from foster mothers set the later phenotypic tone of both RORγ+ Tregs and IgA production. IgA appeared to drive the phenotypes.

We then analyzed *Foxp3-Cre.RORc*$^{fl/fl}$ or *Foxp3-Cre.Ikzf2*$^{fl/fl}$ conditional knockout mice, who are deficient in RORγ+ or Helios+ Tregs, respectively (Thornton et al., 2010; Sefik et al., 2015). Mice deficient in RORγ+ Tregs, but not in Helios+ Tregs, displayed an increase in IgA coating of microbes (Figure 7E). These results, which are consistent with results in c-Maf deficient mice (Neumann et al., 2019), suggest that RORγ+ Tregs also drove the phenotypes.

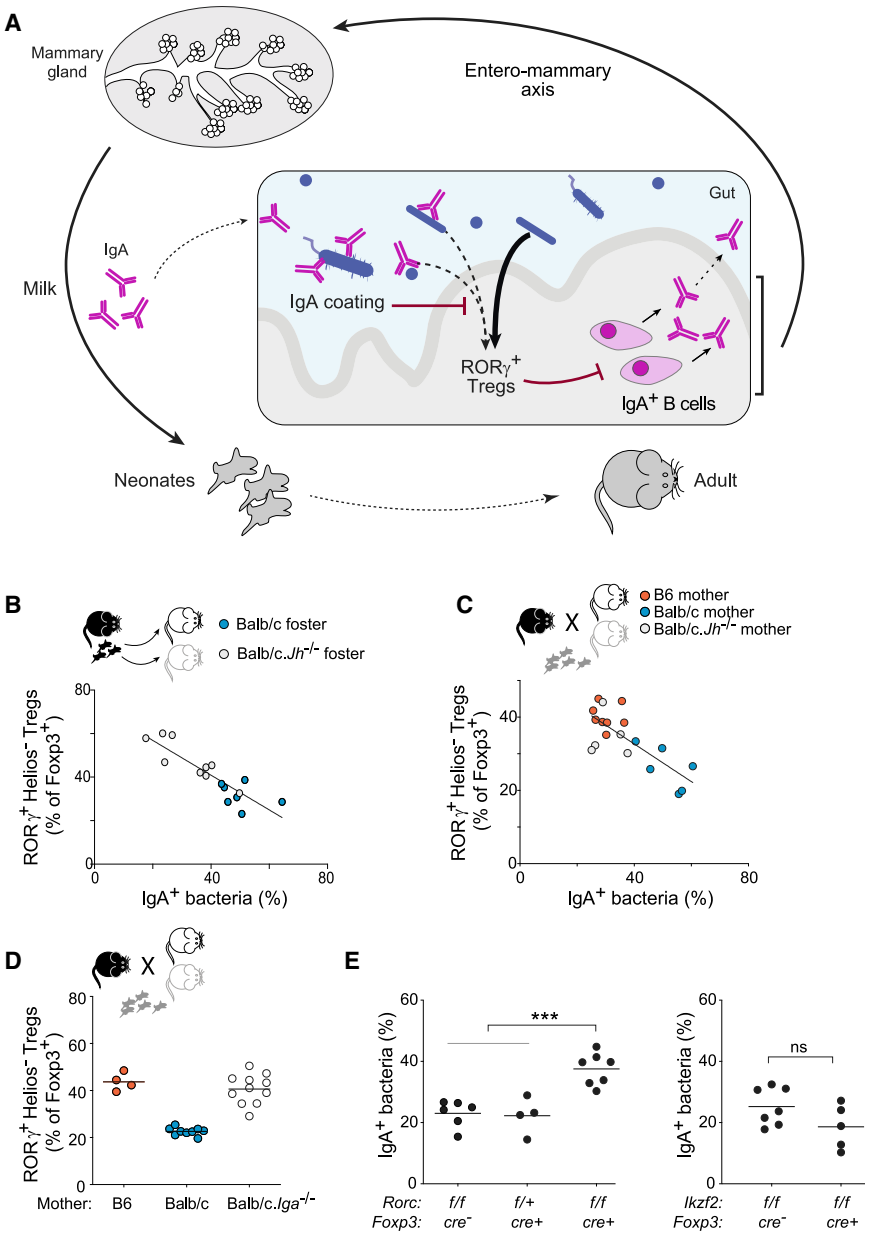

Figure 7. Colonic RORγ+ Tregs and Secretory IgA Regulate Each Other in a Double-Negative Feedback Loop

(A) Proposed model: mothers transfer variable amounts of IgA to their offspring, leading to differences in IgA coating of gut microbes in neonates, which condition RORγ+ Treg proportions in adults, which in turn regulate levels of intestinal IgA+ plasma cells. In female offspring, the resulting IgA differences are reflected in their milk, thus allowing this phenotype to be transferred through multiple generations.

(B) Correlation between proportions of colon RORγ+ Tregs and IgA-coated bacteria in stool of B6 mice fostered by BALB/c or BALB/c.*Jh*−/− mothers at birth.

(C) Correlation between proportions of colon RORγ+ Tregs and IgA-coated bacteria in stool of (B6 × BALB/c)F1 mice born of B6, BALB/c, or BALB/c.*Jh*−/− mothers.

(D) Proportions of colon RORγ+ Tregs in stool of (B6 × BALB/c)F1 mice born of B6, BALB/c, or BALB/c.*Iga*−/− mothers.

(E) Proportions of IgA-coated bacteria in stool of Treg-specific conditional knockout mice deficient in *Rorc* (encodes RORγ) or *Ikzf2* (encodes Helios) and their littermate controls (t test, ***p < 0.001). Data representative of >3 independent experiments, bars in plots indicate mean.

Together, these results validate the double-negative feedback loop between IgA and RORγ+ Tregs, where maternally derived IgA, which preceded both RORγ+ Treg appearance and self-IgA production, initially sets the transmissible balance.

DISCUSSION

We serendipitously discovered that the preponderance of RORγ+ Tregs, an immune cell type crucial for intestinal homeostasis, was quantitatively influenced by the mother. The RORγ+ Treg phenotype was set during a very early and short postnatal window, was stably maintained throughout adulthood, and was passed on by daughters to their offspring for multiple generations. The transmission of the RORγ+ Treg phenotype was not dependent on genetics or epigenetics, nor on transfer of microbiota; instead, it required maternal Ig, and variation in IgA production followed a strikingly similar, but inverse pattern of maternally transmitted and multi-generational heritability.

Integrating these phenomena (influence of the immediate postnatal period but not of gestational mother, carryforward to adult immunocytes that aren't yet present in the imprinted neonate, serial multi-generational transmission of anti-correlated IgA and RORγ+ Treg traits) led us to the model outlined above. Strain-specific maternal transfer of IgA levels via milk in early life leads to differential coating of microbes in the postnatal intestine, which modifies their stimulatory properties and their ability to induce RORγ+ Tregs. In adults, RORγ+ Tregs and IgA+ B cells regulate each other, in a double-negative feedback loop. Finally, when the female mouse becomes pregnant herself, the low or high IgA traits are passed on via milk IgA, which repeats the cycle and ensures multi-generational transmission.

Several examples of the transmission of maternal factors that influence the physiology of the offspring and their later immunologic functions have been described in both mice and humans. Most fundamentally, the mother transmits part of her genome and the epigenetic DNA modifications linked to parental imprinting, or those linked to maternal nutrition (Heard and Martienssen, 2014). Tracing back to Ehrlich's foundational work in

1891 (see Silverstein, 2000), maternal transfer of Igs has long been known to have a major impact on progeny. In a form of passive immunization, maternal Ig protects the neonate against infections, modifies the ability of the offspring to mount immune responses, and may condition autoimmune or allergic disease (Zinkernagel, 2001; Lemke et al., 2004; Bunker and Bendelac, 2018). In the gut, maternal poly-specific IgA limits the penetration of commensal intestinal bacteria, and hence dampens responses against them (Harris et al., 2006; Koch et al., 2016; Bunker and Bendelac, 2018), functions also observed in breast-fed humans (e.g., Gopalakrishna et al., 2019). The mother also contributes microbes and their metabolites, which are essential for early colonization and shaping the local immune system, transplacentally and postnatally (Honda and Littman, 2012; Macpherson et al., 2017). Transmission of microbes from mother to progeny has the potential for multi-generational effects (Sonnenburg et al., 2016). Yet other maternal factors transmitted through milk, such as growth factors or milk polysaccharides, may also modulate responses to microbes in early life by altering trans-epithelial passage or biasing the growth of bacterial species (Knoop et al., 2015; Zivkovic et al., 2011). Of these, which were at play here? Most immediately, genetic and epigenetic transmission, and transplacental effects, were ruled out by the transmission in the first few days of life. That BALB/c and B6 mothers and their female descendants might differentially transmit an RORγ+ Treg-inducing microbe would be compatible with the timing but was largely ruled out by the experiments of Figure 4, and by our inability to find a consistent differential transmission of bacteria that correlates with the Treg phenotype in either neonates or adults. These results are compatible with those of Fransen and colleagues, who only reported a very modest difference in overall diversity between B6 and BALB/c mice (Fransen et al., 2015). Further, it seems implausible that differential passage of a single microbe or genus could possibly lead to the constant difference between F1 progeny, one found in every mouse, and in mice from all colonies, when RORγ+ Treg induction is known to be a widespread trait among gut commensals (Sefik et al., 2015). Similarly, it seems difficult to imagine how a differential propensity of B6 and BALB/c mice to produce milk polysaccharides or growth factors could be transmitted through generations. However, the realization that IgA production in the gut and milk was a mirror image of RORγ+ Treg levels provided a key clue to understand multi-generational transmission.

Our observations, combined with previously reported results, elucidate the mechanisms underlying the various steps of the model. (1) Treg regulation of IgA: such regulation is conceptually straightforward, given these cells' habitual role in dampening the function of other immunocytes and given previous reports that Foxp3-IgA axis is involved in the maintenance of microbial populations and intestinal homeostasis. Paradoxically, these studies reported a positive effect of Tregs on IgA production (Cong et al., 2009; Kawamoto et al., 2014), but they did not discriminate Treg subpopulations, and their interpretation could be complicated by the effect of acute and complete Treg depletion. More recently, in accord with the present findings, mice with c-Maf-deficient Tregs showed increases in colonic IgA+ plasma cells and IgA coating of microbes (Neumann et al., 2019). (2) IgA dampening RORγ Treg cells: coating by IgA modulates how commensals are sensed by the immune system (Bunker et al., 2017; Bunker et al., 2015; Bunker and Bendelac, 2018), and pro-inflammatory species of commensal bacteria are more prone to high IgA coating (Palm et al., 2014). We propose that IgA coating dampens RORγ+ Treg induction and underlies the "return" arm of the IgA < > RORγ+ Treg negative regulatory loop, reflecting several possible mechanisms because stimulatory epitopes on the bacteria would be shielded by IgA (Harris et al., 2006), or because IgA coating could alter the microbes' ability to come into close contact with the mucosa (Donaldson et al., 2018; Uchimura et al., 2018), or because IgA coating can induce transitions in the synthesis of the target epitope, as shown for an IgA monoclonal antibody (mAb) that targets *B. thetaiotamicron* (Peterson et al., 2007). Either (or several) of these mechanisms could dampen RORγ+ Treg induction and the observed differences in T cell activation. (3) Persistence from the neonate to the adult: there is certainly precedent in mucosal immunology for influences on the postnatal immune system that project to adulthood (Olszak et al., 2012; Al Nabhani et al., 2019; Gomez de Agüero et al., 2016; Constantinides et al., 2019), but the conundrum here is that the cells affected (RORγ+ Treg and IgA+ B cells) are not present in the postnatal days when the signal is received. Persistence could be explained by a remnant effect on the microbiota, by stable effects on the gut epithelial, stromal, or neuronal micro-environment, or by the demonstrated ability of maternally derived Ig to influence later immune responses, for instance by biasing specific antigen presentation (Lemke et al., 2004). (4) Information transfer from gut to milk: the last step in the model requires the RORγ+ Treg and IgA setpoints in the gut to be transferred to the mammary gland, such that the cycle can be re-initiated. RORγ+ Tregs themselves can't be the conduit, as they are essentially absent from the lactating mammary gland (data not shown); IgA itself or IgA-producing cells are thus more likely vectors to set IgA levels in the milk. The colonization of the mammary gland by IgA-producing plasma cells of gut origin (Roux et al., 1977; Wilson and Butcher, 2004) as well as transport of circulating IgA from the blood via the pIgR transporter (Johansen and Kaetzel, 2011) have been described, so we assume that these processes will carry-over the transmission of gut-level differences to the milk, and thus to the next generation, ensuring the multi-generational transmission.

Importantly, we are not proposing here that IgA-coating of inducing microbes is the sole regulator of RORγ+ Treg levels. This is an actively researched topic, and several non-mutually exclusive intermediates have been proposed to mediate the impact of the microbiome on RORγ+ Tregs, some more controversially than others: short-chain fatty acids (Arpaia et al., 2013; Furusawa et al., 2013; Smith et al., 2013; Ohnmacht et al., 2015; Al Nabhani et al., 2019), bile acids (Hang et al., 2019; Song et al., 2020), capsular antigens (Verma et al., 2018), and neuronal influences (Yissachar et al., 2017). We suggest that the maternally controlled regulation may come in to modulate these influences, e.g., by fixing the range in which these factors can operate.

Another interesting observation from our study is that over several generations, the genetic influence tended to reset maternal influence, which explains why B6 and BALB/c mice

from three different suppliers showed the same RORγ+ Treg skew. In addition, while BALB/c and B6 offspring responded in the same direction to maternal factors, BALB/c mice never quite reached the RORγ+ Treg levels of B6 mice, and vice versa. Thus, the genetically determined and maternally transmitted factors buffer each other in setting the levels of this key immunoregulatory population. Mice with lower RORγ+ Treg fractions were better protected from intestinal infection, while those with higher proportions were less susceptible to colitis, cancer, and allergy, highlighting the advantage of balancing selection for the trait. From a Darwinian standpoint, IgA and Treg-based transmission allows a more rapid adaptation to environmental variation than DNA-based genetic selection and provides a degree of hysteresis because optimal immunoregulatory balances and adaptation to commensals are preserved between generations. It can thus be seen as an intermediate between genetic selection and the fast but ultimately lost adjustments of an individual's adaptive immune system. Importantly, the resetting of RORγ+ Treg levels after the strong perturbation provoked by DSS was later transmitted to progeny, underscoring that events in one generation can condition immune phenotypes in the next. This resetting was maintained for several weeks after DSS, but it remains to be seen whether, in the real world outside an SPF colony, strong environmental changes might alter the neonatally determined setpoint.

RORγ+ Tregs influence colonic inflammation and cancer and have been implicated in food allergies (Blatner et al., 2012; Abdel-Gadir et al., 2019; Sefik et al., 2015; Ohnmacht et al., 2015; Al Nabhani et al., 2019). Our observations thus have important implications in understanding the heritability of these complex disorders that characteristically have an important heritable component, usually only partially accounted for by genetic variation (Manolio et al., 2009; Jostins et al., 2012). Our results suggest that maternal transfer of RORγ+ Treg setpoints may contribute to "missing heritability." Maternal immunologic transmission could also plausibly partake in the rapid rise in incidence of allergies and autoimmune diseases over the past decades, which are too rapid to be explained by genetic changes (Cho and Gregersen, 2011). These maternal factors would best be factored in for the design and interpretation of GWAS studies.

In summary, this study highlights the non-genetic transfer of an important immunoregulatory trait by immunologic means, for which the entero-mammary axis provides the mechanistic underpinning of multi-generational matrilineal transmission. Several of the model's steps require further exploration, but the multi-generational propagation of RORγ+ Tregs and IgA may be an important tenet when considering the evolution of immune responses and autoimmune diseases.

STAR★METHODS

Detailed methods are provided in the online version of this paper and include the following:

SUPPLEMENTAL INFORMATION

Supplemental Information can be found online at https://doi.org/10.1016/j.cell.2020.04.030.

ACKNOWLEDGMENTS

We thank Drs. J. Huh and H. Cantor for discussions and materials, K. Hattori and F. Chen for help with mice and immunologic analyses, C. Laplace for figures, and K. Bedirian for the pedigree-drawing software. Supported by grants from the NIH, United States (AI125603 and AI051530), by a gift from the Howalt family, and in part by SRAs from UCB and Evelo Biosciences. D.R. was supported by Damon Runyon Cancer Research Foundation, United States (DRG 2300-17, National Mah Jongg League) and S.G.-P. by EMBO, Germany (ALTF 547-2019).

AUTHOR CONTRIBUTIONS

Design, D.R., E.S., D.M., and C.B.; Experimentation, D.R., E.S., and S.G.-P.; Computation, M.W., L.Y., Z.Y., A.K., and C.B.; Writing – Original Draft, D.R., S.G.-P., and C.B.; Writing – Review & Editing, all authors.

DECLARATION OF INTERESTS

The authors declare no competing interests.

Received: October 7, 2019
Revised: January 22, 2020
Accepted: April 17, 2020
Published: May 12, 2020

REFERENCES

Abdel-Gadir, A., Stephen-Victor, E., Gerber, G.K., Noval Rivas, M., Wang, S., Harb, H., Wang, L., Li, N., Crestani, E., Spielman, S., et al. (2019). Microbiota therapy acts via a regulatory T cell MyD88/RORγt pathway to suppress food allergy. Nat. Med. *25*, 1164–1174.

Acha-Orbea, H., and MacDonald, H.R. (1995). Superantigens of mouse mammary tumor virus. Annu. Rev. Immunol. *13*, 459–486.

Al Nabhani, Z., Dulauroy, S., Marques, R., Cousu, C., Al Bounny, S., Déjardin, F., Sparwasser, T., Bérard, M., Cerf-Bensussan, N., and Eberl, G. (2019). A weaning reaction to microbiota is required for resistance to immunopathologies in the adult. Immunity *50*, 1276–1288.e5.

Allis, C.D., and Jenuwein, T. (2016). The molecular hallmarks of epigenetic control. Nat. Rev. Genet. *17*, 487–500.

Arpaia, N., Campbell, C., Fan, X., Dikiy, S., van der Veeken, J., deRoos, P., Liu, H., Cross, J.R., Pfeffer, K., Coffer, P.J., and Rudensky, A.Y. (2013). Metabolites produced by commensal bacteria promote peripheral regulatory T-cell generation. Nature *504*, 451–455.

Barreiro, L.B., and Quintana-Murci, L. (2010). From evolutionary genetics to human immunology: how selection shapes host defence genes. Nat. Rev. Genet. *11*, 17–30.

Baym, M., Kryazhimskiy, S., Lieberman, T.D., Chung, H., Desai, M.M., and Kishony, R. (2015). Inexpensive multiplexed library preparation for megabase-sized genomes. PLoS ONE *10*, e0128036.

Blatner, N.R., Mulcahy, M.F., Dennis, K.L., Scholtens, D., Bentrem, D.J., Phillips, J.D., Ham, S., Sandall, B.P., Khan, M.W., Mahvi, D.M., et al. (2012). Expression of RORγt marks a pathogenic regulatory T cell subset in human colon cancer. Sci. Transl. Med. *4*, 164ra159.

Bolyen, E., Rideout, J.R., Dillon, M.R., Bokulich, N.A., Abnet, C.C., Al-Ghalith, G.A., Alexander, H., Alm, E.J., Arumugam, M., Asnicar, F., et al. (2019). Reproducible, interactive, scalable and extensible microbiome data science using QIIME 2. Nat. Biotechnol. *37*, 852–857.

Brodin, P., Jojic, V., Gao, T., Bhattacharya, S., Angel, C.J., Furman, D., Shen-Orr, S., Dekker, C.L., Swan, G.E., Butte, A.J., et al. (2015). Variation in the human immune system is largely driven by non-heritable influences. Cell *160*, 37–47.

Bunker, J.J., and Bendelac, A. (2018). IgA responses to microbiota. Immunity *49*, 211–224.

Bunker, J.J., Flynn, T.M., Koval, J.C., Shaw, D.G., Meisel, M., McDonald, B.D., Ishizuka, I.E., Dent, A.L., Wilson, P.C., Jabri, B., et al. (2015). Innate and adaptive humoral responses coat distinct commensal bacteria with immunoglobulin A. Immunity *43*, 541–553.

Bunker, J.J., Erickson, S.A., Flynn, T.M., Henry, C., Koval, J.C., Meisel, M., Jabri, B., Antonopoulos, D.A., Wilson, P.C., and Bendelac, A. (2017). Natural polyreactive IgA antibodies coat the intestinal microbiota. Science *358*, eaan6619.

Caporaso, J.G., Lauber, C.L., Walters, W.A., Berg-Lyons, D., Huntley, J., Fierer, N., Owens, S.M., Betley, J., Fraser, L., Bauer, M., et al. (2012). Ultra-high-throughput microbial community analysis on the Illumina HiSeq and MiSeq platforms. ISME J. *6*, 1621–1624.

Cho, J.H., and Gregersen, P.K. (2011). Genomics and the multifactorial nature of human autoimmune disease. N. Engl. J. Med. *365*, 1612–1623.

Collins, J.W., Keeney, K.M., Crepin, V.F., Rathinam, V.A., Fitzgerald, K.A., Finlay, B.B., and Frankel, G. (2014). Citrobacter rodentium: infection, inflammation and the microbiota. Nat. Rev. Microbiol. *12*, 612–623.

Cong, Y., Feng, T., Fujihashi, K., Schoeb, T.R., and Elson, C.O. (2009). A dominant, coordinated T regulatory cell-IgA response to the intestinal microbiota. Proc. Natl. Acad. Sci. USA *106*, 19256–19261.

Constantinides, M.G., Link, V.M., Tamoutounour, S., Wong, A.C., Perez-Chaparro, P.J., Han, S.J., Chen, Y.E., Li, K., Farhat, S., Weckel, A., et al. (2019). MAIT cells are imprinted by the microbiota in early life and promote tissue repair. Science *366*, eaax6624.

Dendrou, C.A., Petersen, J., Rossjohn, J., and Fugger, L. (2018). HLA variation and disease. Nat. Rev. Immunol. *18*, 325–339.

Donaldson, G.P., Ladinsky, M.S., Yu, K.B., Sanders, J.G., Yoo, B.B., Chou, W.C., Conner, M.E., Earl, A.M., Knight, R., Bjorkman, P.J., and Mazmanian, S.K. (2018). Gut microbiota utilize immunoglobulin A for mucosal colonization. Science *360*, 795–800.

Ferretti, P., Pasolli, E., Tett, A., Asnicar, F., Gorfer, V., Fedi, S., Armanini, F., Truong, D.T., Manara, S., Zolfo, M., et al. (2018). Mother-to-Infant Microbial Transmission from Different Body Sites Shapes the Developing Infant Gut Microbiome. Cell Host Microbe *24*, 133–145.e5.

Fransen, F., Zagato, E., Mazzini, E., Fosso, B., Manzari, C., El Aidy, S., Chiavelli, A., D'Erchia, A.M., Sethi, M.K., Pabst, O., et al. (2015). BALB/c and C57BL/6 mice differ in polyreactive IgA abundance, which impacts the generation of antigen-specific IgA and microbiota diversity. Immunity *43*, 527–540.

Franzosa, E.A., McIver, L.J., Rahnavard, G., Thompson, L.R., Schirmer, M., Weingart, G., Lipson, K.S., Knight, R., Caporaso, J.G., Segata, N., and Huttenhower, C. (2018). Species-level functional profiling of metagenomes and metatranscriptomes. Nat. Methods *15*, 962–968.

Furusawa, Y., Obata, Y., Fukuda, S., Endo, T.A., Nakato, G., Takahashi, D., Nakanishi, Y., Uetake, C., Kato, K., Kato, T., et al. (2013). Commensal microbe-derived butyrate induces the differentiation of colonic regulatory T cells. Nature *504*, 446–450.

Geva-Zatorsky, N., Sefik, E., Kua, L., Pasman, L., Tan, T.G., Ortiz-Lopez, A., Yanortsang, T.B., Yang, L., Jupp, R., Mathis, D., et al. (2017). Mining the human gut microbiota for immunomodulatory organisms. Cell *168*, 928–943.e11.

Gomez de Agüero, M., Ganal-Vonarburg, S.C., Fuhrer, T., Rupp, S., Uchimura, Y., Li, H., Steinert, A., Heikenwalder, M., Hapfelmeier, S., Sauer, U., et al. (2016). The maternal microbiota drives early postnatal innate immune development. Science *351*, 1296–1302.

Gopalakrishna, K.P., Macadangdang, B.R., Rogers, M.B., Tometich, J.T., Firek, B.A., Baker, R., Ji, J., Burr, A.H.P., Ma, C., Good, M., et al. (2019). Maternal IgA protects against the development of necrotizing enterocolitis in preterm infants. Nat. Med. *25*, 1110–1115.

Hang, S., Paik, D., Yao, L., Kim, E., Trinath, J., Lu, J., Ha, S., Nelson, B.N., Kelly, S.P., Wu, L., et al. (2019). Bile acid metabolites control T_H17 and T_{reg} cell differentiation. Nature *576*, 143–148.

Harris, N.L., Spoerri, I., Schopfer, J.F., Nembrini, C., Merky, P., Massacand, J., Urban, J.F., Jr., Lamarre, A., Burki, K., Odermatt, B., et al. (2006). Mechanisms of neonatal mucosal antibody protection. J. Immunol. *177*, 6256–6262.

Heard, E., and Martienssen, R.A. (2014). Transgenerational epigenetic inheritance: myths and mechanisms. Cell *157*, 95–109.

Hedrick, P.W. (2007). Balancing selection. Curr. Biol. *17*, R230–R231.

Hirota, K., Turner, J.E., Villa, M., Duarte, J.H., Demengeot, J., Steinmetz, O.M., and Stockinger, B. (2013). Plasticity of Th17 cells in Peyer's patches is responsible for the induction of T cell-dependent IgA responses. Nat. Immunol. *14*, 372–379.

Honda, K., and Littman, D.R. (2012). The microbiome in infectious disease and inflammation. Annu. Rev. Immunol. *30*, 759–795.

Johansen, F.E., and Kaetzel, C.S. (2011). Regulation of the polymeric immunoglobulin receptor and IgA transport: new advances in environmental factors that stimulate pIgR expression and its role in mucosal immunity. Mucosal Immunol. *4*, 598–602.

Jostins, L., Ripke, S., Weersma, R.K., Duerr, R.H., McGovern, D.P., Hui, K.Y., Lee, J.C., Schumm, L.P., Sharma, Y., Anderson, C.A., et al.; International IBD Genetics Consortium (IIBDGC) (2012). Host-microbe interactions have shaped the genetic architecture of inflammatory bowel disease. Nature *491*, 119–124.

Kane, M., Case, L.K., Kopaskie, K., Kozlova, A., MacDearmid, C., Chervonsky, A.V., and Golovkina, T.V. (2011). Successful transmission of a retrovirus depends on the commensal microbiota. Science *334*, 245–249.

Kawamoto, S., Maruya, M., Kato, L.M., Suda, W., Atarashi, K., Doi, Y., Tsutsui, Y., Qin, H., Honda, K., Okada, T., et al. (2014). Foxp3($^+$) T cells regulate immunoglobulin a selection and facilitate diversification of bacterial species responsible for immune homeostasis. Immunity *41*, 152–165.

Kim, S., Kim, H., Yim, Y.S., Ha, S., Atarashi, K., Tan, T.G., Longman, R.S., Honda, K., Littman, D.R., Choi, G.B., and Huh, J.R. (2017). Maternal gut bacteria promote neurodevelopmental abnormalities in mouse offspring. Nature *549*, 528–532.

Knoop, K.A., McDonald, K.G., McCrate, S., McDole, J.R., and Newberry, R.D. (2015). Microbial sensing by goblet cells controls immune surveillance of luminal antigens in the colon. Mucosal Immunol. *8*, 198–210.

Koch, M.A., Reiner, G.L., Lugo, K.A., Kreuk, L.S., Stanbery, A.G., Ansaldo, E., Seher, T.D., Ludington, W.B., and Barton, G.M. (2016). Maternal IgG and IgA antibodies dampen mucosal T helper cell responses in early life. Cell *165*, 827–841.

Lemke, H., Coutinho, A., and Lange, H. (2004). Lamarckian inheritance by somatically acquired maternal IgG phenotypes. Trends Immunol. *25*, 180–186.

Macpherson, A.J., de Agüero, M.G., and Ganal-Vonarburg, S.C. (2017). How nutrition and the maternal microbiota shape the neonatal immune system. Nat. Rev. Immunol. *17*, 508–517.

Manolio, T.A., Collins, F.S., Cox, N.J., Goldstein, D.B., Hindorff, L.A., Hunter, D.J., McCarthy, M.I., Ramos, E.M., Cardon, L.R., Chakravarti, A., et al.

(2009). Finding the missing heritability of complex diseases. Nature *461*, 747–753.

Marrack, P., Kushnir, E., and Kappler, J. (1991). A maternally inherited superantigen encoded by a mammary tumour virus. Nature *349*, 524–526.

McDonald, B., and McCoy, K.D. (2019). Maternal microbiota in pregnancy and early life. Science *365*, 984–985.

Moon, C., Baldridge, M.T., Wallace, M.A., D, C.A., Burnham, Virgin, H.W., and Stappenbeck, T.S. (2015). Vertically transmitted faecal IgA levels determine extra-chromosomal phenotypic variation. Nature *521*, 90–93.

Morton, A.M., Sefik, E., Upadhyay, R., Weissleder, R., Benoist, C., and Mathis, D. (2014). Endoscopic photoconversion reveals unexpectedly broad leukocyte trafficking to and from the gut. Proc. Natl. Acad. Sci. USA *111*, 6696–6701.

Netea, M.G., Wijmenga, C., and O'Neill, L.A. (2012). Genetic variation in Toll-like receptors and disease susceptibility. Nat. Immunol. *13*, 535–542.

Neumann, C., Blume, J., Roy, U., Teh, P.P., Vasanthakumar, A., Beller, A., Liao, Y., Heinrich, F., Arenzana, T.L., Hackney, J.A., et al. (2019). c-Maf-dependent T_{reg} cell control of intestinal T_H17 cells and IgA establishes host-microbiota homeostasis. Nat. Immunol. *20*, 471–481.

Ohnmacht, C., Park, J.H., Cording, S., Wing, J.B., Atarashi, K., Obata, Y., Gaboriau-Routhiau, V., Marques, R., Dulauroy, S., Fedoseeva, M., et al. (2015). MUCOSAL IMMUNOLOGY. The microbiota regulates type 2 immunity through RORγ^+ T cells. Science *349*, 989–993.

Olszak, T., An, D., Zeissig, S., Vera, M.P., Richter, J., Franke, A., Glickman, J.N., Siebert, R., Baron, R.M., Kasper, D.L., and Blumberg, R.S. (2012). Microbial exposure during early life has persistent effects on natural killer T cell function. Science *336*, 489–493.

Palm, N.W., de Zoete, M.R., Cullen, T.W., Barry, N.A., Stefanowski, J., Hao, L., Degnan, P.H., Hu, J., Peter, I., Zhang, W., et al. (2014). Immunoglobulin A coating identifies colitogenic bacteria in inflammatory bowel disease. Cell *158*, 1000–1010.

Peterson, D.A., McNulty, N.P., Guruge, J.L., and Gordon, J.I. (2007). IgA response to symbiotic bacteria as a mediator of gut homeostasis. Cell Host Microbe *2*, 328–339.

Pratama, A., Schnell, A., Mathis, D., and Benoist, C. (2020). Developmental and cellular age direct conversion of CD4$^+$ T cells into RORγ^+ or Helios$^+$ colon Treg cells. J. Exp. Med. *217*, e20190428.

Purdy, A., Case, L., Duvall, M., Overstrom-Coleman, M., Monnier, N., Chervonsky, A., and Golovkina, T. (2003). Unique resistance of I/LnJ mice to a retrovirus is due to sustained interferon gamma-dependent production of virus-neutralizing antibodies. J. Exp. Med. *197*, 233–243.

Roux, M.E., McWilliams, M., Phillips-Quagliata, J.M., Weisz-Carrington, P., and Lamm, M.E. (1977). Origin of IgA-secreting plasma cells in the mammary gland. J. Exp. Med. *146*, 1311–1322.

Schiering, C., Krausgruber, T., Chomka, A., Fröhlich, A., Adelmann, K., Wohlfert, E.A., Pott, J., Griseri, T., Bollrath, J., Hegazy, A.N., et al. (2014). The alarmin IL-33 promotes regulatory T-cell function in the intestine. Nature *513*, 564–568.

Sefik, E., Geva-Zatorsky, N., Oh, S., Konnikova, L., Zemmour, D., McGuire, A.M., Burzyn, D., Ortiz-Lopez, A., Lobera, M., Yang, J., et al. (2015). MUCOSAL IMMUNOLOGY. Individual intestinal symbionts induce a distinct population of RORγ^+ regulatory T cells. Science *349*, 993–997.

Sharon, G., Cruz, N.J., Kang, D.W., Gandal, M.J., Wang, B., Kim, Y.M., Zink, E.M., Casey, C.P., Taylor, B.C., Lane, C.J., et al. (2019). Human Gut Microbiota from Autism Spectrum Disorder Promote Behavioral Symptoms in Mice. Cell *177*, 1600–1618.e17.

Silverstein, A.M. (2000). The most elegant immunological experiment of the XIX century. Nat. Immunol. *1*, 93–94.

Smith, P.M., Howitt, M.R., Panikov, N., Michaud, M., Gallini, C.A., Bohlooly-Y, M., Glickman, J.N., and Garrett, W.S. (2013). The microbial metabolites, short-chain fatty acids, regulate colonic Treg cell homeostasis. Science *341*, 569–573.

Solomon, B.D., and Hsieh, C.S. (2016). Antigen-Specific Development of Mucosal Foxp3+RORγt+ T Cells from Regulatory T Cell Precursors. J. Immunol. *197*, 3512–3519.

Song, X., Sun, X., Oh, S.F., Wu, M., Zhang, Y., Zheng, W., Geva-Zatorsky, N., Jupp, R., Mathis, D., Benoist, C., and Kasper, D.L. (2020). Microbial bile acid metabolites modulate gut RORγ^+ regulatory T cell homeostasis. Nature *577*, 410–415.

Sonnenburg, E.D., Smits, S.A., Tikhonov, M., Higginbottom, S.K., Wingreen, N.S., and Sonnenburg, J.L. (2016). Diet-induced extinctions in the gut microbiota compound over generations. Nature *529*, 212–215.

Thornton, A.M., Korty, P.E., Tran, D.Q., Wohlfert, E.A., Murray, P.E., Belkaid, Y., and Shevach, E.M. (2010). Expression of Helios, an Ikaros transcription factor family member, differentiates thymic-derived from peripherally induced Foxp3+ T regulatory cells. J. Immunol. *184*, 3433–3441.

Tomura, M., Yoshida, N., Tanaka, J., Karasawa, S., Miwa, Y., Miyawaki, A., and Kanagawa, O. (2008). Monitoring cellular movement in vivo with photoconvertible fluorescence protein "Kaede" transgenic mice. Proc. Natl. Acad. Sci. USA *105*, 10871–10876.

Uchimura, Y., Fuhrer, T., Li, H., Lawson, M.A., Zimmermann, M., Yilmaz, B., Zindel, J., Ronchi, F., Sorribas, M., Hapfelmeier, S., et al. (2018). Antibodies Set Boundaries Limiting Microbial Metabolite Penetration and the Resultant Mammalian Host Response. Immunity *49*, 545–559.e5.

Verma, R., Lee, C., Jeun, E.J., Yi, J., Kim, K.S., Ghosh, A., Byun, S., Lee, C.G., Kang, H.J., Kim, G.C., et al. (2018). Cell surface polysaccharides of *Bifidobacterium bifidum* induce the generation of Foxp3$^+$ regulatory T cells. Sci. Immunol. *3*, eaat6975.

Wilson, E., and Butcher, E.C. (2004). CCL28 controls immunoglobulin (Ig)A plasma cell accumulation in the lactating mammary gland and IgA antibody transfer to the neonate. J. Exp. Med. *200*, 805–809.

Xu, M., Pokrovskii, M., Ding, Y., Yi, R., Au, C., Harrison, O.J., Galan, C., Belkaid, Y., Bonneau, R., and Littman, D.R. (2018). c-MAF-dependent regulatory T cells mediate immunological tolerance to a gut pathobiont. Nature *554*, 373–377.

Yassour, M., Jason, E., Hogstrom, L.J., Arthur, T.D., Tripathi, S., Siljander, H., Selvenius, J., Oikarinen, S., Hyöty, H., Virtanen, S.M., et al. (2018). Strain-Level Analysis of Mother-to-Child Bacterial Transmission during the First Few Months of Life. Cell Host Microbe *24*, 146–154.e4.

Yatsunenko, T., Rey, F.E., Manary, M.J., Trehan, I., Dominguez-Bello, M.G., Contreras, M., Magris, M., Hidalgo, G., Baldassano, R.N., Anokhin, A.P., et al. (2012). Human gut microbiome viewed across age and geography. Nature *486*, 222–227.

Ye, C.J., Feng, T., Kwon, H.K., Raj, T., Wilson, M.T., Asinovski, N., McCabe, C., Lee, M.H., Frohlich, I., Paik, H.I., et al. (2014). Intersection of population variation and autoimmunity genetics in human T cell activation. Science *345*, 1254665.

Ye, J., Qiu, J., Bostick, J.W., Ueda, A., Schjerven, H., Li, S., Jobin, C., Chen, Z.E., and Zhou, L. (2017). The aryl hydrocarbon receptor preferentially marks and promotes gut regulatory T cells. Cell Rep. *21*, 2277–2290.

Yissachar, N., Zhou, Y., Ung, L., Lai, N.Y., Mohan, J.F., Ehrlicher, A., Weitz, D.A., Kasper, D.L., Chiu, I.M., Mathis, D., and Benoist, C. (2017). An intestinal organ culture system uncovers a role for the nervous system in microbe-immune crosstalk. Cell *168*, 1135–1148.e12.

Zinkernagel, R.M. (2001). Maternal antibodies, childhood infections, and autoimmune diseases. N. Engl. J. Med. *345*, 1331–1335.

Zivkovic, A.M., German, J.B., Lebrilla, C.B., and Mills, D.A. (2011). Human milk glycobiome and its impact on the infant gastrointestinal microbiota. Proc. Natl. Acad. Sci. USA *108* (*Suppl 1*), 4653–4658.

STAR★METHODS

KEY RESOURCES TABLE

REAGENT or RESOURCE	SOURCE	IDENTIFIER
Antibodies		
Anti-mouse CD45 Brilliant Violet 605	Biolegend	Cat#103140; RRID: AB_2562342
Anti-mouse CD45 Pacific blue	Biolegend	Cat#103126; RRID: AB_493535
Anti-mouse CD45 APC Cy7	Biolegend	Cat#103116; RRID: AB_312981
Anti-mouse CD45 Brilliant Violet 510	Biolegend	Cat#103138; RRID: AB_2563061
Anti-mouse CD4 Alexa 700	Biolegend	Cat#100430; RRID: AB_493699
Anti-mouse CD4 FITC	Biolegend	Cat#100406; RRID: AB_312691
Anti-mouse CD4 APC Cy7	Biolegend	Cat#100414; RRID: AB_312699
Anti-mouse CD4 BV 605	Biolegend	Cat#100451; RRID: AB_2564591
Anti-mouse CD4 PerCP Cy5.5	Biolegend	Cat#100434; RRID: AB_893324
Anti-mouse CD8a Alexa 700	Biolegend	Cat#100730; RRID: AB_493703
Anti-mouse TCRβ chain PE Cy7	Biolegend	Cat#109222; RRID: AB_893625
Anti-mouse TCRβ chain Pacific blue	Biolegend	Cat#109226; RRID: AB_1027649
Anti-mouse TCRβ chain FITC	Biolegend	Cat#109206; RRID: AB_313429
Anti-mouse TCRδ chain PE Cy7	Biolegend	Cat#118124; RRID: AB_11204423
Anti-mouse CD19 APC Cy7	Biolegend	Cat#115530; RRID: AB_830707
Anti-mouse B220 PE-Cy7	Biolegend	Cat# 103222; RRID: AB_313005
Anti-mouse/human CD11b PerCP Cy5.5	Biolegend	Cat#101228; RRID: AB_893232
Anti-mouse CD11c APC Cy7	Biolegend	Cat#117324; RRID: AB_830649
Anti-mouse Ly6c FITC	Biolegend	Cat#128006; RRID: AB_1186135
Anti-mouse CD103 Pacific blue	Biolegend	Cat#121418; RRID: AB_2128619
Anti-mouse F4/80 Alexa 700	Biolegend	Cat#123130; RRID: AB_2293450
Anti-mouse CD137(PDCA-1) Alexa Fluor 647	Biolegend	Cat#127106; RRID: AB_2067120
Anti-mouse CX3CR1 APC	Biolegend	Cat#149008; RRID: AB_2564492
Anti-mouse I-A/I-E (MHCII) Biotin	Biolegend	Cat#107604; RRID: AB_313319
Brilliant Violet 711 Streptavidin	Biolegend	Cat#405241
Anti-mouse CD185 (CXCR5) PerCP Cy5.5	Biolegend	Cat#145508; RRID: AB_2561972
Anti-mouse PD-1 PE Cy7	Biolegend	Cat#135216; RRID: AB_10689635
Anti-mouse CD80 FITC	Biolegend	Cat#104706; RRID: AB_313127
Anti-mouse CD86 PE	Biolegend	Cat#159203; RRID: AB_2832567
Anti-mouse NK1.1 APC Cy7	Biolegend	Cat#108724; RRID: AB_830871
Anti-mouse/human CD44 FITC	Biolegend	Cat#103006; RRID: AB_312957
Anti-mouse CD69 APC Cy7	Biolegend	Cat#104526; RRID: AB_10679041
Anti-mouse Ly6a/e (Sca-1) Alexa 700	Biolegend	Cat#108142; RRID: AB_2565959
Anti-mouse CD62L PE	Biolegend	Cat#104408; RRID: AB_313095
Anti-mouse IL17A APC	Biolegend	Cat#506916; RRID: AB_536018
Anti-mouse IFNγ FITC	Biolegend	Cat#505806; RRID: AB_315400
Anti-mouse IL10 Pacific blue	Biolegend	Cat#505020; RRID: AB_2125094
Anti-mouse IL22 PE	Biolegend	Cat#516404; RRID: AB_2124255
Anti-mouse Helios Pacific blue	Biolegend	Cat#137220; RRID: AB_10690535
Anti-mouse/rat Foxp3 APC	Invitrogen	Cat#17-5773-82; RRID: AB_469457
Anti-mouse Foxp3 PerCP Cy5.5	Invitrogen	Cat#45-5773-82; RRID: AB_914351
Anti-mouse/human ROR gamma (t) PE	Invitrogen	Cat#12-6988-80; RRID: AB_1257212
Anti-mouse/human ROR gamma (t) APC	Invitrogen	Cat#17-6988-82; RRID: AB_10609207

(*Continued on next page*)

Continued

REAGENT or RESOURCE	SOURCE	IDENTIFIER
Anti-mouse/human Gata3 Alexa 488	Invitrogen	Cat#53-9966-42; RRID: AB_2574493
Anti-mouse c-Maf PE	Invitrogen	Cat#12-9855-42; RRID: AB_2572747
Anti-Mouse IgG, Fcγ fragment specific Alexa fluor 647	Jackson Immunoresearch	Cat#115-605-071
Anti-mouse IgA PE	Invitrogen	Cat#12-4204-83; RRID: AB_465918
Anti-mouse IgA Dylight 650	Bethyl Laboratories	Cat#A90-103D5; RRID: AB_10630982
Anti-gp36TM monoclonal antibody	Purdy et al., 2003	N/A
Anti-gp52 monoclonal antibody	Purdy et al., 2003	N/A
Bacterial and Virus Strains		
Bacteroides thetaiotamicron	Geva-Zatorsky et al.,2017	N/A
Clostridium ramosum	Geva-Zatorsky et al.,2017	N/A
Peptostreptococcus magnus	Geva-Zatorsky et al.,2017	N/A
Citrobacter rodentium	ATCC	ATCC 51459
Chemicals, Peptides, and Recombinant Proteins		
Dextran Sodium Sulfate	Affymetrix	Cat#14489
Oxytocin	Sigma-Aldrich	Cat#O4375-250IU
Collagenase, Type II (GIBCO)	Thermo Fisher Scientific	Cat#17101015
Dispase (GIBCO)	Thermo Fisher Scientific	Cat#17105-041
BD GolgiPlug, Protein Transport Inhibitor	BD	Cat#555029
Ionomycin	Sigma-Aldrich	Cat#I0634
Phorbol 12-Myristate 13-acetate (PMA)	Sigma-Aldrich	Cat# P8139
Bacto Yeast Extract (for PYG broth)	Thermo Fisher Scientific	Cat#212750
Bacto Proteose Peptone No.3 (for PYG broth)	Thermo Fisher Scientific	Cat#211693
Luria-Bertani broth	BD	Cat#244520
MacConkey Agar	Fisher Scientific	Cat#B11387
BBL Brucella Agar with 5% Sheep Blood	Fisher Scientific	Cat#BD297848
Metronidazole	Sigma-Aldrich	Cat#M1547
Ampicillin	Sigma-Aldrich	Cat#A0166
Neomycin	Fisher Scientific	Cat#BP2669-25
Vancomycin	RPI	Cat#1404-93-9
Diphtheria toxin	Sigma-Aldrich	Cat#D0564
Kapa 2x HiFi HotStart PCR mix	Kapa Biosystems	Cat#KK2601
Ampure XP beads	Beckman Coulter	Cat#A63881
Critical Commercial Assays		
Mouse IgA ELISA kit	Invitrogen	Cat#88-50450-86
DNeasy Powersoil kit	QIAGEN	Cat#12888-100
eBioscience Transcription Factor Staining Buffer Set	Thermo Fisher Scientific	Cat#50-112-8857
Live/Dead BacLight Bacterial Counting and Viability kit	Invitrogen	Cat#L34856
Illumina Tagment DNA Enzyme and Buffer Kit	Illumina	Cat#20034197
QIAquick PCR Purification Kit	QIAGEN	Cat#28183
Deposited Data		
Metagenomics data	This paper	Available at NCBI accession # PRJNA614518
16S sequencing data	This paper	Available at NCBI accession # PRJNA610699
Experimental Models: Organisms/Strains		
B6 SPF mice	Jackson Laboratory	000664-C57BL/6J
B6 SPF mice	Taconic Farms	C57BL/6NTac
B6 SPF mice	Charles River	C57BL/6NCrl

(*Continued on next page*)

Continued

REAGENT or RESOURCE	SOURCE	IDENTIFIER
BALB/c SPF mice	Jackson Laboratory	000651-Balb/cJ
BALB/c SPF mice	Taconic Farms	BALB/cAnNTac
BALB/c SPF mice	Charles River	BALB/cAnNCrl
BALB/c *Jh*−/− mice	Taconic Farms	*Igh-J*^{tm1Dhu} N?+N2
CBA/J	Jackson Laboratory	000656-CBA/J
NOD	Jackson Laboratory	001976-NOD/ShiLtJ
B6 Rorcfl/fl Foxp3-gfp-cre mice	Sefik et al., 2015	N/A
B6 Ikzf2fl/fl Foxp3-gfp-cre mice	This paper	N/A
BALB/c *IgA*−/− mice	Kasper lab	N/A
B6 Kaede mice	Tomura et al., 2008 Morton et al., 2014	N/A
Germ Free mice	GF C57BL/6 colony housed in the animal facility at Harvard Medical School.	C57BL/6
Oligonucleotides		
Primers used for 16S sequencing	This paper (Table S2)	N/A
Primers used for metagenomic analysis	This paper (Table S2)	N/A
Software and Algorithms		
FlowJo 10	BD	https://www.flowjo.com
Prism 8	GraphPad	https://www.graphpad.com/scientific-software/prism/
QIIME2	Bolyen et al., 2019	https://qiime2.org
FastQC	Babraham Bioinformatics	https://www.bioinformatics.babraham.ac.uk/projects/fastqc/
KneadData	Huttenhower lab	http://huttenhower.sph.harvard.edu/kneaddata
HUMAnN2	Franzosa et al., 2018	http://huttenhower.sph.harvard.edu/humann
Other		
Double electric breast-pump	Lansinoh	N/A
Lysing Matrix D tubes	MP Biomedicals	Cat#116913100
Electra Pro Series Violet Handheld Laser pointer	Laserglow Technologies	N/A
Fiberoptic endoscope	ZIBRA Corporation	N/A

LEAD CONTACT AND MATERIALS AVAILABILITY

Further information and requests for resources and reagents should be directed to and will be fulfilled by the Lead Contact Prof. Christophe Benoist (cbdm@hms.harvard.edu). This study did not generate new unique reagents.

EXPERIMENTAL MODEL AND SUBJECT DETAILS

Mice

C57BL/6, and BALB/c mice were purchased from Jackson, Taconic, and Charles River, CBA/J, and NOD mice were purchased from Jackson, and were maintained in specific pathogen free conditions at Harvard Medical School. *Jh*−/− mice on the BALB/c background were purchased from Taconic, *IgA*−/− mice were obtained from D. Kasper and bred in our facility to generate wild-type and homozygous littermate controls for use as mothers. *Rorc*$^{fl/fl}$ Foxp3-cre mice were bred and maintained in our facility. *Ikzf2*$^{fl/fl}$ mice were obtained from H. Cantor and were crossed to Foxp3-gfp-cre in our facility. Kaede reporter mice were obtained from O. Kanagawa (RIKEN, Wako, Japan) and maintained on the B6 background (Tomura et al., 2008; Morton et al., 2014).

For strain intercross experiments, F1 mice were generated by crossing B6 males and females with BALB/c females and males respectively. F1 crosses of NODxCBA, B6xCBA, NODxBalb/c, and Kaede F1 (B6xBalb/c) were generated similarly. For backcross experiments, F1 females born to B6 mothers were chosen at random and crossed to BALB/c males. Female offspring of every subsequent generation were chosen at random and crossed to BALB/c males. The RORγ+ Treg phenotype of each backcrossed

generation was determined from littermates of the breeding females. Backcross of F1 females born to BALB/c mothers were generated by crossing every generation to B6 males. All experiments, unless otherwise specified in the text, were performed in mice of mixed gender at six weeks of age.

For cross-fostering experiments, pups were given foster moms at birth before the appearance of milk spots in their stomach. Generally, a single litter of pups was split between the test foster mother and the control foster mother. The pups to be fostered were gently placed in dirty bedding and nesting of the foster mother to transfer her scent and then placed with the foster mother. The foster pups were monitored for signs of rejection, in which case the pups were euthanized. B6 and BALB/c germ-free mice were bred and maintained in our facility at Harvard Medical School. All experiments were performed following guidelines listed in animal protocols IS00000187 and IS00001257, approved by Harvard Medical School's Institutional Animal Care and Use Committee.

METHOD DETAILS

Mice treatment, infection, and colonization

For mono-colonization, GF mice were orally gavaged with single bacterial species at 4 weeks of age for 2 weeks. Stool was collected and plated at 2 weeks to verify colonization and rule out contamination from other species. For infection, six-week-old mice were orally gavaged with 1×10^9 *cf.*u of *C. rodentium* resuspended in 100 μL PBS. Bacterial density was confirmed by dilution plating. Stool was collected routinely to monitor colonization and bacterial clearance. For DTR experiments, six-week-old mice were injected intra-peritoneally with two doses of 20ng/g of diphtheria toxin, followed by four weeks of recovery. For DSS-colitis, mice on the B6 background were treated with 2.5% DSS for 6 days in their drinking water followed by 4 days of recovery. Inter-strain F1 mice were not susceptible to 2.5% DSS as measured by weight loss or changes in colon length, consistent with previously described strain dependent susceptibility to this model. Hence, F1 mice were given 4% DSS in their drinking water for 6 days and their colons were analyzed at day 10. For antibiotics treatment, mice were treated with 0.5mg/mL vancomycin (RPI), 1mg/mL metronidazole (Sigma-Aldrich), 1mg/mL neomycin (Fisher Scientific), 1mg/mL ampicillin (Sigma-Aldrich) (VMNA) dissolved in drinking water for three weeks. Mothers were treated with VMNA from E12.5 or E15.5 to E17.5 for B6 mice, and E14 or E17 to E19 for BALB/c mice, so both groups of mothers received no antibiotics in their last day of gestation to minimize the transfer of antibiotics in their milk. All antibiotic treated mothers were given foster pups and their own pups were euthanized to rule out any effect of antibiotics during gestation.

Milking mice

The mother is separated from her litter for 3 h prior to milking. Pups were maintained in a warm nesting environment during this time. The mothers were anesthetized using an isoflurane machine and were kept under isoflurane for the entire duration of milking. The mothers were injected with 0.1 mL (2 IU) of oxytocin intraperitoneally two minutes before the start of milking and each individual teat was cleaned with alcohol pads. Mothers were milked using a home-made apparatus, with modified tubing attached to a store-bought double electric breast pump (Lansinoh) under the lowest settings. Milk collected was stored in the refrigerator for upto 3 days for immediate gavage experiments or frozen at −20 for ELISAs.

Bacteria

For mono-colonization experiments, *B. thetaiotamicron*, *P. magnus*, and *C. rodentium* were all grown in BBL brucella blood agar plates, followed by overnight standing cultures in PYG broth under strictly anaerobic conditions (80% N_2, 10% H_2, 10% CO_2) at 37°C in an anaerobic chamber. For infection, *C. rodentium* was first grown on MacConkey Agar plates, followed by overnight cultures in Luria-Bertani broth with shaking at 37°C. The overnight culture was then diluted to an optical density of 0.1 followed by an additional 4 h of growth.

Preparation of lymphocytes and flow cytometry

Intestinal tissues were measured, cleaned, and treated with RPMI containing 1 mM DTT, 20 mM EDTA and 2% FBS at 37C for 15 min to remove epithelial cells, minced and dissociated in collagenase solution (1.5mg/mL collagenase II (GIBCO), 0.5mg/mL dispase and 1%FBS in RPMI) with constant stirring at 37C for 40min. Single cell suspensions were filtered and washed with 10% RPMI solution.

Lymphocytes from spleen, bone marrow, and Peyer's patches were obtained by mechanical disruption, followed by red blood cell lysis, and filtered and washed with 10% RPMI solution.

The resulting cells were stained with different panels of antibodies with surface markers for CD45, CD4, CD8, TCR-β, TCR-δ, NK1.1, B220, IgA, CD19, CD11c, CD11b, Ly6c, PDCA-1, F4/80, CD103, CX3CR1, CD80, CD86, MHCII, CD44, CD62L, CD69, Sca-1, CXCR5, and PD-1 (Biolegend), and intracellular markers for RORγ, FoxP3, c-Maf, Gata3 (eBioscience), Helios, IL17a, IFNγ, IL10, and IL-22 (Biolegend). For cytokine analysis, cells were treated with RMPI containing 10% FBS, 30ng/mL phorbol 12-myristate 13-acetate (Sigma), 1 μM Ionomycin (Sigma) in presence of GolgiStop (BD Biosciences) for 3.5 h. For intracellular staining of cytokines and transcription factors, cells were stained for surface markers and fixed in eBioscience Fix/Perm buffer overnight, followed by permeabilization in eBioscience permeabilization buffer at room temperature for 45 min in the presence of antibodies. Cells were acquired with a BD LSRFortessa or BD FACSymphony and analysis was performed with FlowJo 10 software.

IgA/IgG coating and IgA ELISA

For bacterial coating, fecal pellets were homogenized in PBS, filtered, and centrifuged to collect the bacterial fraction. This fraction was washed in PBS+1% BSA, blocked with normal rat serum, and stained with anti-IgA (eBioscience) and anti-IgG (Jackson Immunoresearch). Cells were washed and resuspended in PBS with SYTO 9 (Bacterial counting kit, Invitrogen) and analyzed by FACS. Total IgA was measured using the mouse IgA ELISA kit from Invitrogen.

Analysis of cell migration in the Kaede system

Mice were anesthetized with ketamine:xylazine in combination (10 mg/kg:2 mg/kg i.p). For photoconversion of Kaede in small intestine, mouse abdomen was shaved with peanut trimmers and disinfected by triple application of betadine disinfectant alternating with 70% alcohol prior to surgery. Mice were placed on their backs with an aluminum foil blanket covering all but the shaved area, and a longitudinal 2 cm incision was made in the skin and the peritoneum to expose the intestines. Violet light (Electra Pro Series Violet Handheld Laser pointer, 405 nm, peak power < 5 mW, 3mm diameter; Laserglow Technologies) was shone onto the exposed area of the intestine for 5 s/in. Peritoneum incision is closed using chromic absorbable sutures and skin incision is closed using 6-0 Sofsilk.

For cell photoconversion in the descending colon, a custom-built fiberoptic endoscope (ZIBRA Corporation) was coupled to the handheld 405-nm laser, via an in-house, custom-made connection device (fixed mounts were purchased from ThorLabs). After cleansing the colon of fecal pellets with PBS, we inserted the fiberoptic endoscope through the anus into the descending colon to a depth of 2.5 cm. The laser was switched on, thereby exposing the inner colon to violet light (beam diameter was 3.5 mm). Subsequently, the endoscope was gently retracted, pausing at 2-mm increments for 30 s light pulses at each interval (for a total of 5 min). We estimate that this procedure allows us to photoconvert about two-fifths of the small intestine and colon combined.

Capture ELISA to detect MMTV

Viral fractions were isolated from milk samples. Purified anti-gp52 mAbs of the IgG1 isotype (Purdy et al., 2003) were bound to plastic at 3 g/mL followed by incubation with virions collected from the mouse milk via spinning through 30% sucrose cushion (Kane et al., 2011). ELISA was developed with anti–gp36TM mAb (Purdy et al., 2003) coupled to biotin followed by incubation with streptavidin horseradish peroxidase.

Bacterial population profiling

16S sequencing

DNA was isolated from neonate and adult stool samples using phenol/chloroform and the QIAquick PCR purification kit (QIAGEN). For 16S rDNA profiling, the V4 region of 16S rRNA gene was amplified with primers 515F and 806R (Caporaso et al., 2012), and ~390-bp amplicons were purified and then subjected to multiplex sequencing (Illumina MiSeq, 251 nt x 2 pair-end reads with 12 nt index reads, all primer sequences listed in Table S2). Raw sequencing data were processed with QIIME2 pipelines (Bolyen et al., 2019). In brief, raw sequencing data were imported to QIIME2 and demultiplexed, then DADA2 were used for sequence quality control and feature table construction. The feature table were further used for taxonomic analysis and differential abundance testing.

Metagenomic analysis

DNA was isolated from neonate and adult stool samples using the DNAeasy PowerSoil kit (QIAGEN). Sequencing libraries were prepared using a plate-based method as described in (Baym et al., 2015), where DNA samples were first tagmented with Nextera tagment DNA enzyme (TDE1)(Illumina), and then multiplexed using Kapa 2x HiFi HotStart PCR mix and dual-index primers (Illumina TruSeq primers S502, S503, S505, S506, S507, S508, S510, S511, N701, N702, N703, N704, N705, N706, N707, N710, N711, N712, N714, N715, all primer sequences listed in Table S2). Libraries were cleaned using Ampure XP beads and sequenced on the Illumina NextSeq 500 platform with 150 bp paired-end reads. Samples with low sequence quality were removed by FastQC (https://www.bioinformatics.babraham.ac.uk/projects/fastqc/) and the contaminant reads from human and/or PhiX genomes were filtered out by KneadData (http://huttenhower.sph.harvard.edu/kneaddata). Next, the reads were aligned to their pangenomes and the taxonomic and functional profiles were identified by HUMAnN2 (Franzosa et al., 2018).

QUANTIFICATION AND STATISTICAL ANALYSIS

Data were routinely presented as mean ± SD. Unless stated otherwise, significance was assessed by Student's t test or Mann-Whitney using GraphPad Prism 8.0.

For 16S sequencing, differential representation was evaluated in R, by comparing the mean frequency within each group, or the fraction of positive mice, and estimating the significance of the difference by a Kolmogorov-Smirnoff test and Bonferroni correction. Randomization was used to validate the nominal p values while preserving the cage-effects in the experimental design: which mouse pairs born from the same cage were randomly assigned to the B6 or BALB/c-derived groups, and the same comparisons performed. To parse the relative contribution of shared cage-of-origin versus shared maternal genotype (Figure S3B) Unifrac distances calculated by QIIME2 were compared between all mice and plotted and averaged according to the degree of sharing.

For metagenomic analysis, the taxonomy and pathway comparisons were performed by the Kolmogorov–Smirnov test with FDR adjusted p values.

DATA AND CODE AVAILABILITY

The accession number for the 16S raw data reported in this paper is NCBI Bioproject: PRJNA610699. The accession number for the metagenomics data reported in this paper is NCBI Bioproject:PRJNA614518. OTU tables for both datasets can be found in Table S2.

Supplemental Figures

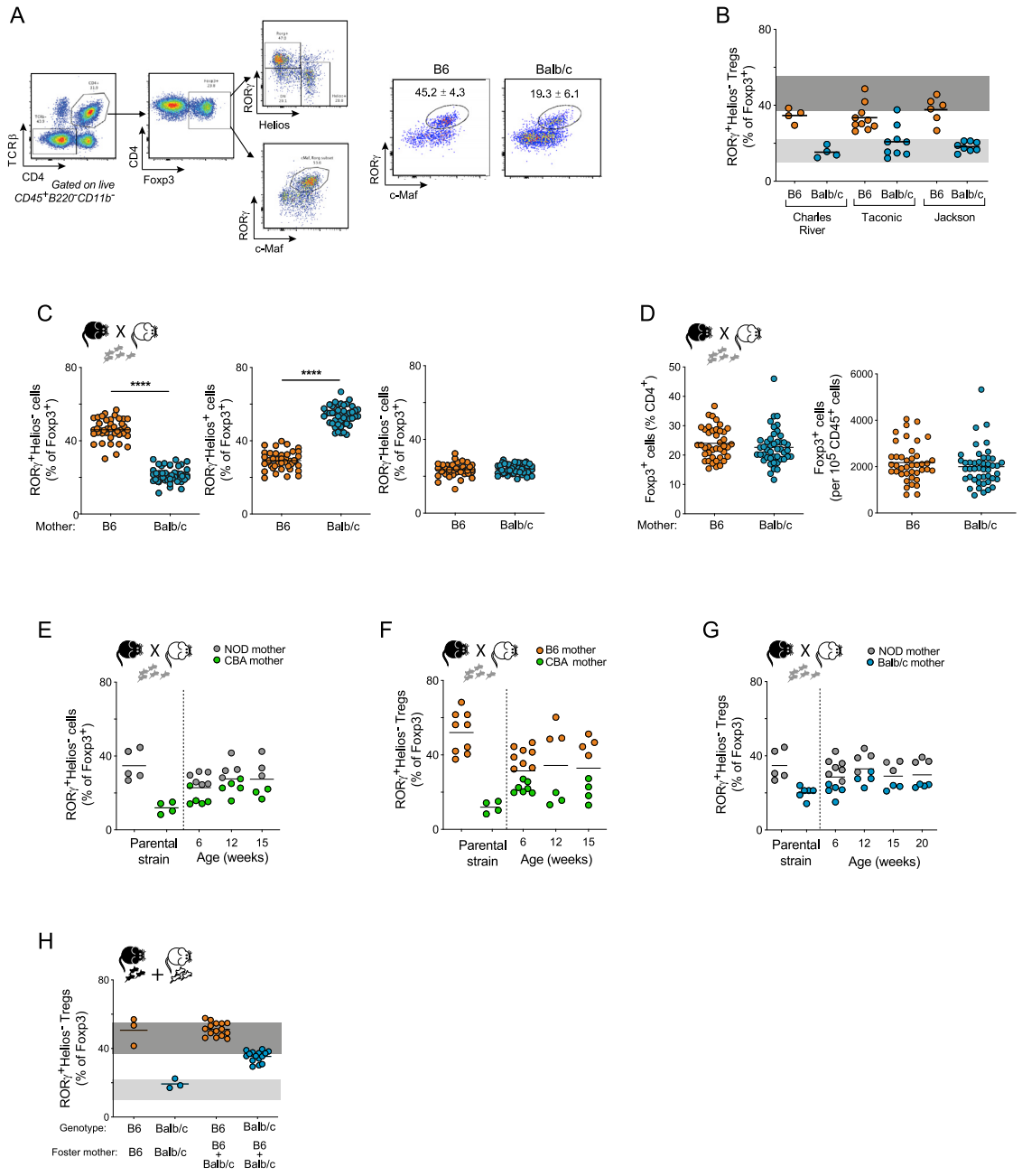

Figure S1. Characterization of Colonic Treg Proportions in Inbred Strains and F1 Mice, Related to Figure 1

A. Representative flow cytometry plots of the gating strategy used to analyze colonic Treg subsets (left), and proportions of colonic RORγ+ versus c-Maf+ Tregs in B6 and BALB/c mice (right).

B. Proportions of RORγ+ Tregs in B6 and BALB/c mice purchased from different facilities / vendors.

C. Quantification of RORγ+ Tregs (left), Helios+ Tregs (middle), RORγ- Helios- Tregs (right) in F1 offspring of B6 and BALB/c mothers (****t test $p < 0.0001$).

D. Quantification of proportions and cell numbers of Foxp3+ Tregs in F1 mice of B6 and BALB/c mothers.

E-G. Proportions of RORγ+ Tregs in F1 offspring resulting from (E) intercross between NOD and CBA strains, (F) intercross between B6 and CBA strains, and (G) NOD and BALB/c strains, at different ages in adulthood.

H. Pregnant B6 and BALB/c mothers were housed together from their last day of gestation until weaning and pups of both genotypes were nursed by both mothers. Quantification of RORγ+ Tregs in B6 and BALB/c mice that were co-housed since birth.

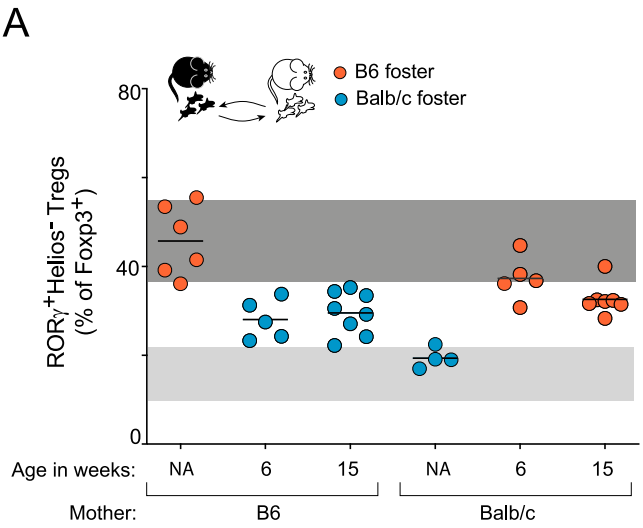

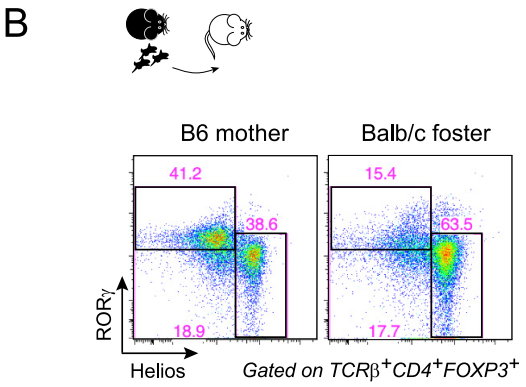

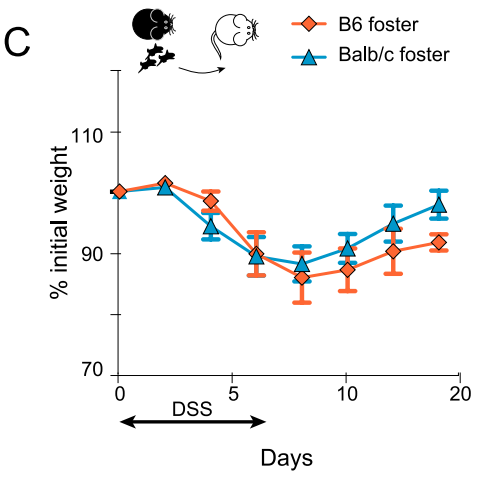

(legend on next page)

Figure S2. Stability of RORγ+ Tregs Is Maintained in Cross-Fostered Mice, Related to Figure 3

A. Proportions of RORγ+ Tregs in B6 mice fostered by BALB/c mothers at birth, BALB/c pups fostered by B6 mothers at birth. Littermates analyzed at 6 weeks and 15 weeks of adulthood.

B. Representative flow cytometry plots of RORγ versus Helios in Foxp3^{DTR} mice fostered by B6 or BALB/c mothers post recovery from DT treatment.

C. Weight loss curve in B6 mice fostered by B6 or BALB/c mothers at birth and treated with 2.5% DSS.

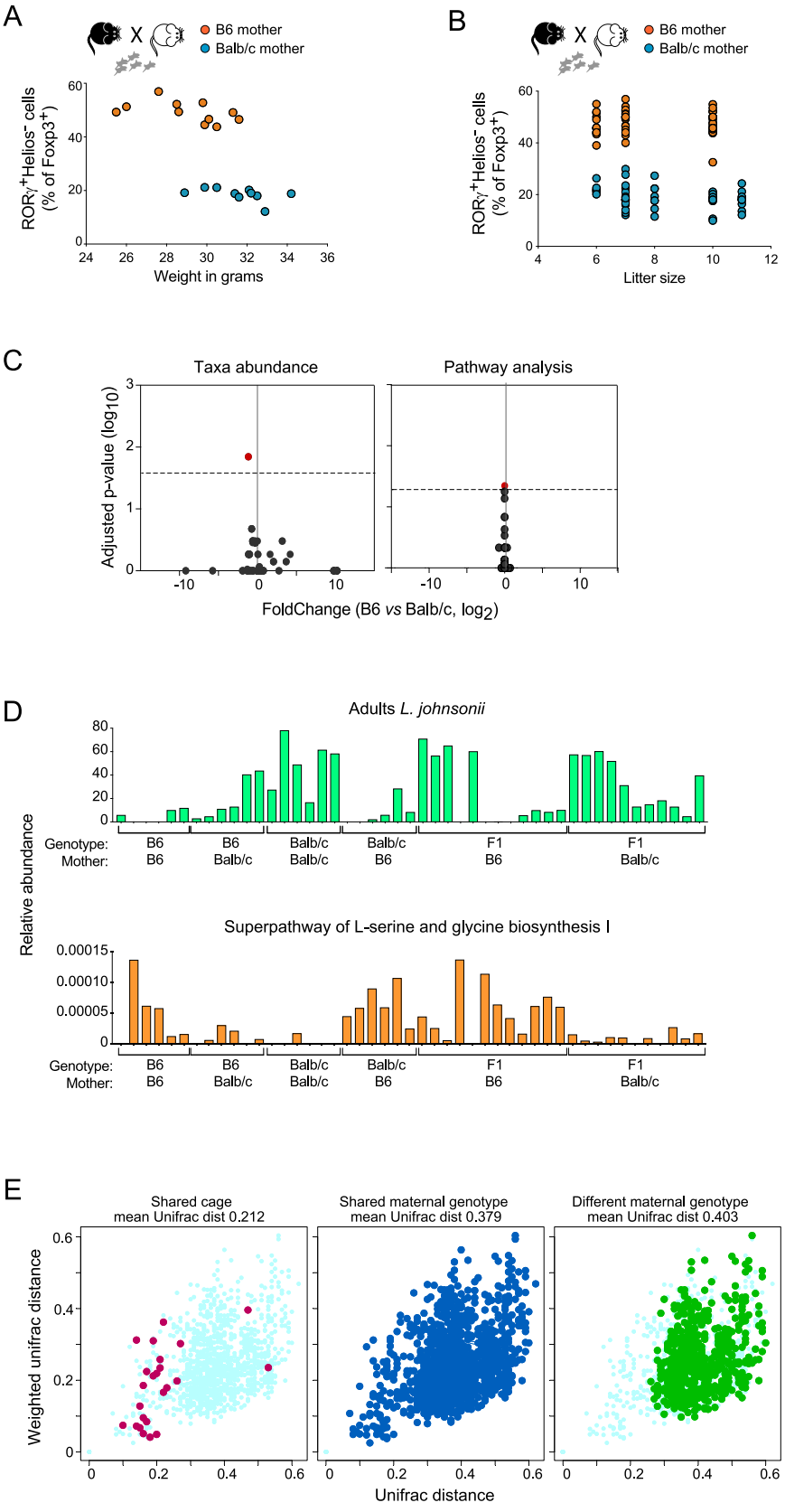

(legend on next page)

Figure S3. RORγ+ Treg Proportions Is Not Determined by Nutritional Factors or Specific Microbial Taxa, Related to Figure 4

A-B. Proportions of RORγ+ Tregs versus mouse weight (A), and litter size (B) of F1 mice born to B6 or BALB/c mothers.

C-D. Regression analysis of individual bacterial taxa (left) or bacterial pathways (right) (C), and relative abundance of indicated bacterial species (top) and pathway (bottom) (D) in stool of 6-week old F1 mice born to B6 or BALB/c mothers, and B6 and BALB/c mice fostered by BALB/c and B6 mothers, and their controls.

E. Cage-of-origin versus genotype influences in stool microbiota of 6-week old F1 mice from B6 or BALB/c mothers (data from Figure 4F). Pairwise UNIFRAC distances (weighted or unweighted) were calculated between all samples (light blue dots in each panel). Left, distances between mice that originate from the same breeding cage. Middle, distances between mice that share the same maternal genotype (but from parallel breeding cages); Right, distances between mice that have different maternal genotypes (B6 versus BALB/c). Wilcoxon rank sum test p.value < 10^{-9} between any group.

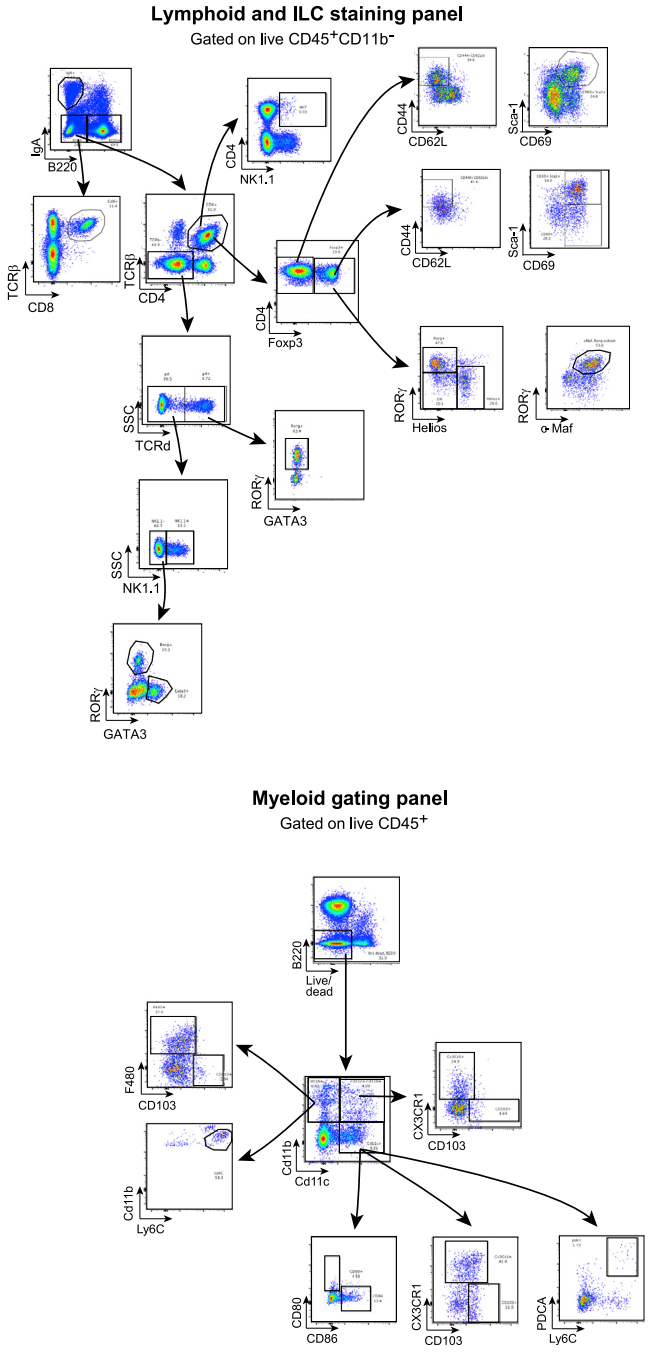

Figure S4. Gating Strategy Used to Profile Colonic Immune Cell Populations in F1 Mice, Related to Figure 5
Representative flow cytometry plots of the analysis used to identify specific ILC, lymphoid and myeloid populations.

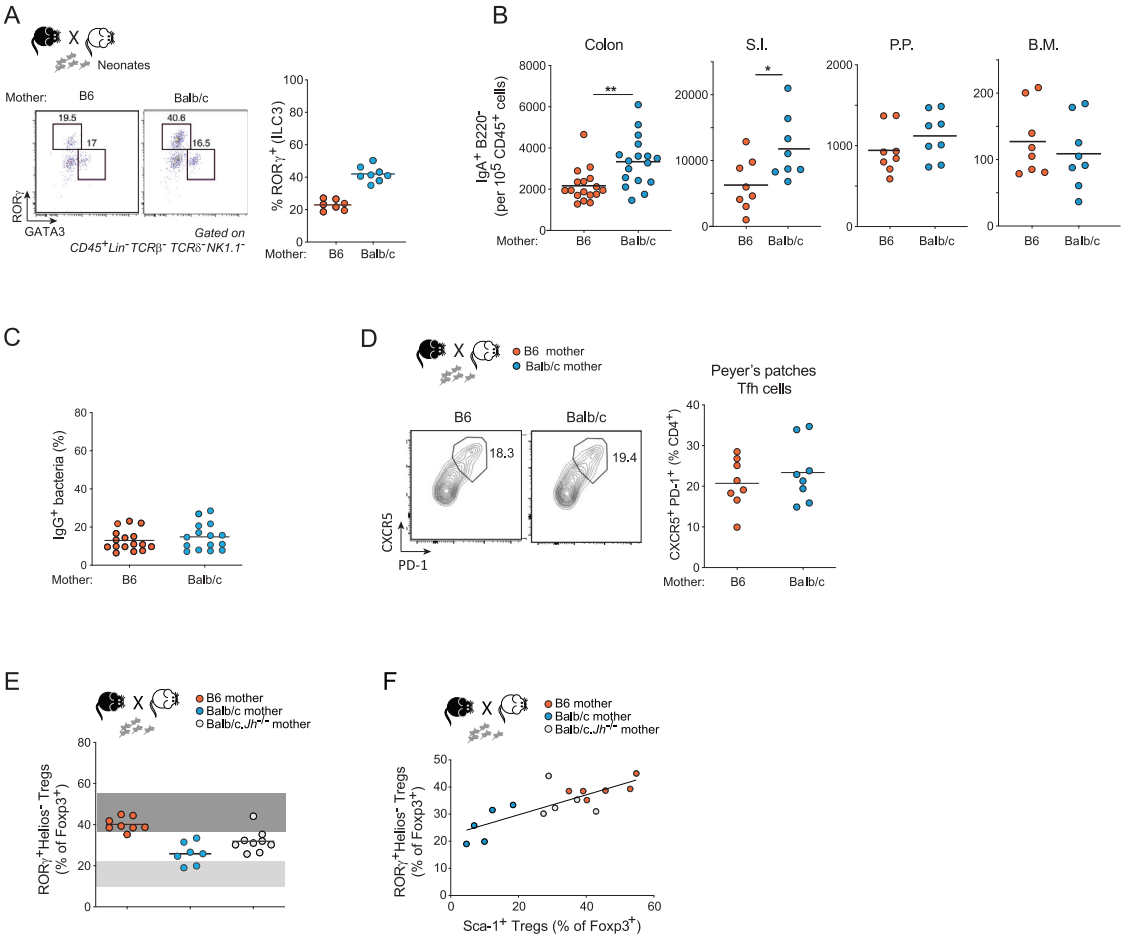

Figure S5. Characterization of Specific Immune Cell Populations in F1 Mice Reveal that IgA+ Plasma Cell Difference Is Restricted to the Intestine, and T Cell Activation States Are Dependent on IgA, Related to Figure 5

A. Representative flow plots and quantification of colonic ILC3 population in neonatal (day 3) F1 mice born to B6 or BALB/c mothers.

B. Quantification of IgA+ plasma cell numbers (normalized to CD45+ cells) in the colon (**t test $p < 0.01$), small intestine (*t test $p < 0.05$), Peyer's patches, and bone marrow of adult F1 mice born to B6 or BALB/c mothers.

C. Quantification of IgG-coated bacteria in stool of adult F1 mice born to B6 or BALB/c mothers.

D. Representative flow plots and quantification of T-follicular helper cells in the Peyer's patches of adult F1 mice born to B6 or BALB/c mothers.

E. Proportions of RORγ+ Tregs in F1 mice born to B6, BALB/c, or BALB/c.*Jh*−/− mothers.

F. Correlation between proportions of colon RORγ+ Treg and Sca1+ Tregs in F1 mice born to either B6, BALB/c, or BALB/c.*Jh*−/− mothers.